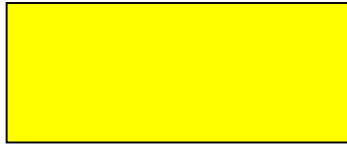




EUROPEAN COMMISSION

**5th EURATOM FRAMEWORK PROGRAMME 1998-2002
KEY ACTION : NUCLEAR FISSION**



**HTR FUEL TECHNOLOGY STUDIES
COMPLEMENTARY ACTIVITIES TO HTR-F**

**CONTRACT N°
FIKI-CT-2001-00150**

**First qualification report of the ATLAS code
on HFR-K3 and FRJ-K15 experiments**

**David MARTIN (BNFL)
Heinz WERNER (FZJ)
Pierre GUILLERMIER (FRAMATOME)
Frédéric MICHEL (CEA)
Guy DEGENEVE (CEA) ;
Mayeul PHELIP (CEA)**

Dissemination level: RE
Document Number: HTR-F1-05/10-D-3.3.1
Draft
Deliverable Number: 3.3

SYNTHESIS

1. CONTENT

This documents presents calculations made with STRESS3 and ATLAS code to simulate the FRJ2-K15/2 and HFR-K3/1 experiments. This two chosen experiment have a very different ratio fluence/FIMA.

Experiment	End FIMA (-)	End Fluence (fast (E>16fJ) neutrons/m ²)	ratio fast fluence/FIMA
FRJ2-K15/2	15.3%	0.2 10 ²⁵	1.31*10 ²⁵
HFR-K3/1	7.5%	4.10 ²⁵	5.33*10 ²⁶

Table of FIMA and fluence at end of experiments

Detail data for this experiments are given by the document :

Nabielek Heinz, Karl Verfondern & Werner Heinz : "Selection of benchmark cases for mechanical failure prediction". HTR-F1-04/08-D-3.1.1 on Sinter Base.

The comparison of the codes results and to the experimental results will permit to increase confidence in ATLAS results.

This document is constituted by the following contributions :

- **BNFL contribution :**
David G. MARTIN. "A benchmark modelling of irradiation HFR K3 and FRJ2 K15"
- **Framatome ANP contribution :**
Lucile DANIEL. "A benchmark modelling of irradiation FRJ2-K15 by ATLAS code"
- **CEA contribution :**
Mayeul PHELIP, Guy DEGENEVE. "HTR-F1 Project – Contribution to deliverable n°3.3 HFR-K3 calculation with ATLAS code".

2. SIMULATION RESULTS FOR EXPERIMENT FRJ2-K15/2

In this experiment, in which the ratio fast fluence/FIMA is very low, the pyrocarbon (PyC) layers, and particularly the buffer PyC layer don't shrink enough to let free space for kernel swelling. In both ATLAS and STRESS3 codes simulations, the kernel arrives in contact with buffer and internal dense PyC layer, generating a highly increasing tensile stress in SiC layer. If we consider the Buffer as rigid, it is followed by a sure silicon carbide (SiC) layer failure.

As no failure occurred in the experimental irradiation, discussions occurred about solutions to remedy to that. One possibility is to decrease or eliminate mechanical interaction trough buffer by reducing its Young modulus or increasing its shrinkage rate. Framatome document presents both results with very low buffer young Modulus or multiplication of fluence to avoid interaction.

When no interaction occurs, calculations show that the SiC layer stresses remains largely negative, leading to no failure.

3. SIMULATION RESULTS FOR EXPERIMENT HFR-K3/1

In this experiment closer to real industrial HTR, the mean particle has the following classical behaviour :

- PyC shrinkage creates rapidly a tensile stress in PyC layers which compress the SiC layer
- As the internal pressure increases, the SiC stress increases. SiC stress decrease up to about 1% FIMA and then increases slowly.

In this experiment, the stresses in SiC remain negative (compression) and failure probability of the mean particle is null.

The failure probability on the particle statistical population, according to given data, is given by STAPPLE calculation in BNFL contribution. It remains null (below 10^{-6}) up to 7,5% FIMA. It is in agreement with the experimental result who shown zero failure on the limited sample of particles.

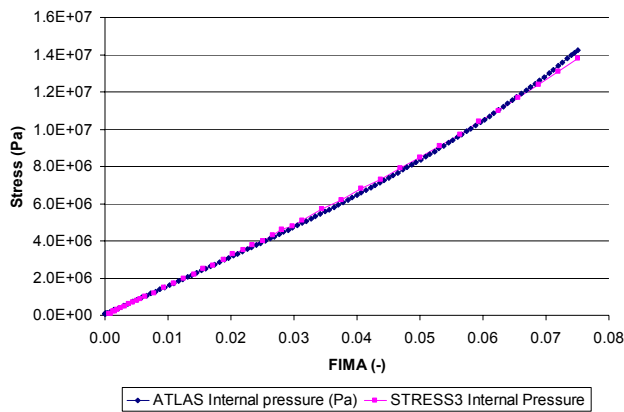
4. CODE COMPARISONS ON HFR-K3/1:

With ATLAS code, it is possible to give diverse models for each of the phenomena. As we see in CEA document, results obtained with so called FZJ, BNFL and CEGA layers properties are sensibly different although the stress evolutions keep following the classical behaviour described above.

If ATLAS uses BNFL properties, then it fits the results of STRESS3 code, except for internal pressure because gas release models differs between STRESS3 and ATLAS default. If we use a appropriate release rate to retrieve STRESS3 pressure, then we can compare precisely the stresses, see figures on next page, and they are almost the same.

5. CONCLUSION

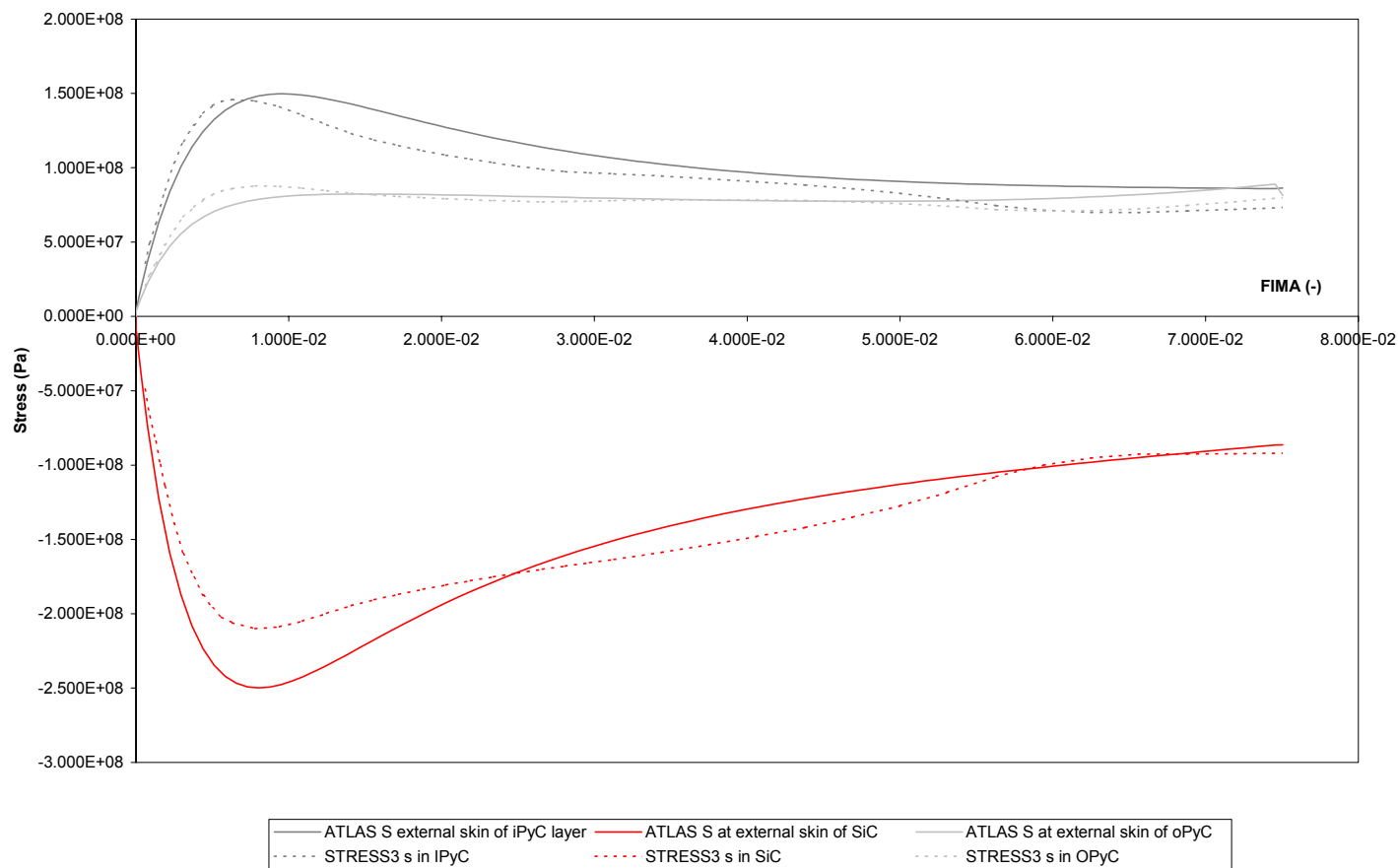
ATLAS permit to retrieve expected behaviour and results. As most of material behaviour are not precisely known, the results given by the code are very uncertain but they correspond to actual (poor) knowledge of particle behaviour under irradiation. This two simulation cases are far to constitute a base for experimental qualification, the more so as both experimental failure fraction (what we try to retrieve) are 0.



'GARR' 0 '==' 1.
'OPF' 0 '*' 2.6

Lines added to ATLAS data file (see
CEA contribution) to retrieve
STRESS3 pressure.

Evolution of pressure for ATLAS and STRESS3 simulation
HFR-K3 experiment



Evolution of tangential stresses in ATLAS and STRESS3 simulations
HFR-K3 experiment

A Benchmark Modelling of Irradiations HFR K3 and FRJ2 K15

David G. Martin[¶]

Consultant to British Nuclear Fuels plc

The codes STRESS3 and STAPLE were employed to model irradiations HFR K3 and FRJ2 K15. Stresses in the SiC layer at the end of the irradiation were respectively very low and very high, the latter being contrary to observation. Possible reasons to explain this discrepancy are advanced.

1. Introduction

At the HTR-F WP3 meeting held at Cadarache on December 1st 2003 participants were invited to model the irradiations HFR K3 and FRJ2 K15 as a means of comparing the results from different codes. This follows on from a previous comparison of the STRESS3 and ATLAS codes reported previously relating to irradiation HFR P4 ⁽¹⁾.

Details of the input data employed in the current exercise are presented in Table 1 ⁽²⁾. Note that throughout this report all stresses are in units of Kgf/cm², temperatures in °C, particle dimensions in microns and neutron doses in units of Dido Nickel Equivalent (to convert from doses >0.1 MeV to Dido Nickel Equivalent values multiply by 0.6). Material property values employed in the calculations were identical to the ones employed previously in STRESS3/STAPLE calculations ⁽³⁾.

2. Results

2.1. HFR K3

Table 2 shows the output data obtained from a STRESS3 run during which the fracture stress of all layers were made unrealistically high in order to avoid the occurrence of any coating failures.

[¶] Nuclear Fuels Consultant, 63 Foliat Drive, Wantage, Oxon OX12 7AL. U.K.
Tel: +44 1235 764754; e-mail: martin@63foliat.freemove.co.uk

Table 1: Specifications of the Particles

Parameter	HFR K3	FRJ2 K15
Kernel Diameter	497±10.3	501±19.8
Buffer thickness	94±14.3	92±14.3
IPyC thickness	41±4	38±3.4
SiC thickness	36±1.7	33±1.9
OPyC thickness	40±2.2	41±3.8
Irradiation temp.	1100	1100
Final burn-up	7.5%	15.3%
Final neutron dose	2.4×10^{25}	1.2×10^{24}

The data presented in Table 2 are shown graphically in Figs. 1–3.

Table 2: Numerical Data from the STRESS3 Run for HFR K3

Dose	Burn-up	σ in IPyC	σ in SiC	σ in OPyC	Pressure	Voidage	Gap(μ m)
0.2	0.06	358	-490	208	1	52.68	1.38
0.3	0.09	496	-671	285	1	52.82	1.84
0.4	0.13	624	-840	356	2	52.95	2.25
0.5	0.16	741	-997	421	2	53.08	2.62
0.6	0.19	849	-1141	482	3	53.21	3.03
0.8	0.25	1033	-1391	586	4	53.46	3.72
1	0.31	1178	-1594	669	5	53.71	4.37
1.2	0.38	1288	-1754	735	6	53.95	4.96
1.4	0.44	1366	-1874	784	7	54.18	5.51
1.6	0.5	1417	-1962	819	8	54.4	6.07
1.8	0.56	1447	-2023	844	9	54.61	6.57
2	0.63	1459	-2061	860	10	54.8	7.03
2.5	0.78	1449	-2101	877	12	55.25	8.09
3	0.94	1410	-2089	875	15	55.67	9.01
3.5	1.09	1353	-2050	862	17	56.03	9.79
4	1.25	1289	-1997	845	20	56.34	10.52
4.5	1.41	1230	-1946	828	22	56.61	11.12
5	1.56	1186	-1905	817	25	56.86	11.63
5.5	1.72	1148	-1869	807	27	57.08	12.08
6	1.88	1114	-1836	799	30	57.28	12.5
6.5	2.03	1084	-1806	791	33	57.46	12.87
7	2.19	1058	-1778	785	35	57.61	13.19

7.5	2.34	1034	-1752	779	38	57.75	13.46
8	2.5	1010	-1726	774	40	57.87	13.69
8.5	2.66	989	-1701	769	43	57.98	13.88
9	2.81	973	-1679	772	46	58.07	14.01
9.5	2.97	966	-1657	775	48	58.15	14.15
10	3.13	959	-1635	778	51	58.22	14.24
11	3.44	944	-1587	782	57	58.33	14.38
12	3.75	926	-1536	783	62	58.4	14.47
13	4.06	906	-1480	782	68	58.42	14.52
14	4.38	884	-1420	778	73	58.41	14.47
15	4.69	858	-1351	770	79	58.36	14.34
16	5	828	-1275	759	85	58.27	14.2
17	5.31	790	-1184	741	91	58.15	14.01
18	5.63	745	-1078	718	97	57.99	13.83
19	5.94	714	-1001	707	104	57.79	13.6
20	6.25	700	-952	710	110	57.55	13.33
21	6.56	698	-927	722	117	57.27	13.05
22	6.88	709	-926	746	124	56.96	12.77
23	7.19	720	-924	771	131	56.62	12.45
24	7.5	732	-921	798	138	56.23	12.08
25	7.81	742	-916	826	146	55.8	11.72
26	8.13	753	-909	856	154	55.32	11.3
27	8.44	763	-900	884	162	54.78	10.89
28	8.75	772	-888	911	171	54.21	10.38
29	9.06	781	-875	935	180	53.59	9.93
30	9.38	790	-861	956	189	52.95	9.37
31	9.69	798	-845	975	199	52.3	8.87
32	10	806	-826	991	209	51.63	8.32
33	10.31	812	-803	1005	220	50.96	7.77
34	10.63	816	-775	1016	230	50.28	7.26
35	10.94	818	-744	1025	242	49.6	6.71
36	11.25	820	-708	1032	253	48.93	6.16

Because stresses in the SiC layer are so modest - indeed compressive when mean particle specifications are employed - one expects very low failure fractions to be observed. This is indeed the case when a STAPLE calculation is performed, employing 10^6 STRESS3 runs, with a mean fracture stress of 4000Kg/cm^2 and $m = 7$. The results are shown in Table 3.

2.2 FRJ2 K15

Table 4 shows the output from a STRESS3 run, while Table 5 the corresponding failure fraction as a function of the burn-up. All this data, apart from that relating to gas gaps are shown in Figs. 4, 5 and 6.

Table 3: Cumulative Failures in HFR K3

Fraction Failed $\times 10^{-5}$	Up to Burn-up %
0.1	9.25
0.3	9.50
0.6	9.75
1.0	10.00
1.4	10.25
2.1	10.50
2.6	10.75
3.2	11.00
3.9	11.25

Table 4: Numerical Data from the STRESS3 Run for FRJ2 K15

Dose	Burn-up	σ in IPyC	σ in SiC	σ in OPyC	Pressure	Voidage	Gap(μm)
0	0	41	82	40	0	51.7	0.45
0.1	1.27	200	-212	128	23	50.51	0.09
0.2	2.55	316	271	229	48	50.11	0
0.3	3.82	411	979	329	74	49.75	0
0.4	5.1	491	1711	423	101	49.4	0
0.5	6.37	555	2468	510	130	49.05	0
0.6	7.65	603	3251	591	160	48.71	0
0.8	10.2	656	4874	732	224	48.06	0
1	12.75	653	6597	848	293	47.42	0
1.2	15.3	602	8329	940	366	46.81	0

Table 4: Numerical Data from the STRESS3 Run for FRJ2 K15

Burn-up	Fraction Failed
2.25	2.00E-06
2.5	6.00E-06
2.75	4.20E-05
3	1.52E-04
3.25	4.28E-04
3.5	9.76E-04
3.75	2.01E-03
4	3.72E-03

4.25	6.53E-03
4.5	1.11E-02
4.75	1.74E-02
5	2.60E-02
5.25	3.75E-02
5.5	5.22E-02
5.75	7.05E-02
6	9.23E-02
6.25	1.18E-01
6.5	1.47E-01
6.75	1.79E-01
7	2.15E-01
7.25	2.53E-01
7.5	2.93E-01
7.75	3.35E-01
8	3.79E-01
8.25	4.23E-01
8.5	4.66E-01
8.75	5.09E-01
9	5.51E-01
9.25	5.91E-01
9.5	6.30E-01
9.75	6.66E-01
10	7.00E-01
10.25	7.32E-01
10.5	7.63E-01
10.75	7.92E-01
11	8.17E-01
11.25	8.41E-01
11.5	8.62E-01
11.75	8.81E-01
12	8.97E-01
12.25	9.12E-01
12.5	9.24E-01
12.75	9.36E-01
13	9.45E-01
13.25	9.54E-01
13.5	9.61E-01
13.75	9.68E-01
14	9.73E-01
14.25	9.78E-01
14.5	9.82E-01
14.75	9.85E-01
15	9.87E-01
15.25	9.90E-01
15.5	9.90E-01

3. Discussion

Experimentally ⁽⁴⁾ it was found that failure fractions in both irradiations were in the region of 10^{-5} , i.e. experimental and modelling results are in good agreement in the case of HFR K3, whereas the calculation grossly over-predicts failures in FRJ2 K15.

The low failure fractions predicted in HFR K3 is understandable, given the modest burn-up and accompanying gas pressure values (Fig. 2). As a result, the SiC layer in a particle with mean specifications is always under compression (Fig. 1).

The remainder of this discussion will be confined to the lack of agreement between calculation and observation in the case of FRJ2 K15.

The major problem in modelling FRJ2 K15 is the very low final fast neutron dose (1.2×10^{24} n/m²) and the comparative (compared with an HTR) low value of the ratio *fast neutron dose / burn-up* value and referred to subsequently as α .

In the first place, at low doses dimensional change rates in the PyC layers are comparatively high and vary significantly with dose. However, the main problem is how the buffer layer should be modelled. In particular, we can only guess values for the dimensional change rates and elastic constants and how they vary with neutron dose.

In the present calculations, kernel-coating mechanical interaction (KCMI) occurs almost from the start of the irradiation. This is mainly because of the low α value, in particular because, at this stage, the buffer layer will have densified very little. In STRESS3 the densification is assumed (guessed) to take place over the dose range $0 - 15 \times 10^{24}$ n/m², and by the end of life in this particular irradiation only about one fifth of the overall densification will have taken place. By contrast, with HTR α values the full extent of the densification will be able to occur and a significant burn-up to have been achieved before the onset of KCMI. On the other hand, should the densification of the buffer occur to its full extent over a much smaller neutron dose interval this would delay the onset of KCMI in the FRJ2 K15, thereby decreasing failure fraction values.

The other area of uncertainty is in knowing what values to take for the elastic modulus of the buffer layer. In STRESS3 it is assumed to be half the corresponding pyrocarbon value. Perhaps in the case of irradiations with HTR α values this assumption is satisfactory because the buffer will have densified to the full extent,

before the onset of KCMI. However, with very low α values, when KCMI will be initiated prior to substantial densification, perhaps the corresponding elastic modulus should be considerably reduced.

In the light of this discussion it would appear that because of these problems relating to the buffer input data, experiment FRJ2 K15 is not a very appropriate irradiation on which to perform a benchmark exercise. Of course, such problems could be overcome in such an exercise if all participants were to employ identical material property values and any consideration of whether or not the results bore any resemblance to experimental reality ignored.

Perhaps one positive conclusion that emerges from the above discussion is the desirability to perform irradiations under conditions where their α values are comparable to those in an HTR.

Acknowledgement

The support of British Nuclear Fuels plc for the work presented here is gratefully acknowledged.

References

1. D. G. Martin. Modelling the HFR-P4 irradiation. A comparison between results from STRESS3 and STAPLE.
2. K. Verfondern. e-mail to D. G. Martin, 3 June 2004.
3. D. G. Martin. Physical and mechanical properties of the constituents of coated fuel particles and the effect of irradiation. Paper presented at HTR-F WP3 meeting, Lyon 18 October 2001.
4. K. Verfondern (editor) Fuel performance and fission product behaviour in gas cooled reactors. IAEA-TECDOC 978 (1997) Section 3.4.2.1.

June 2004

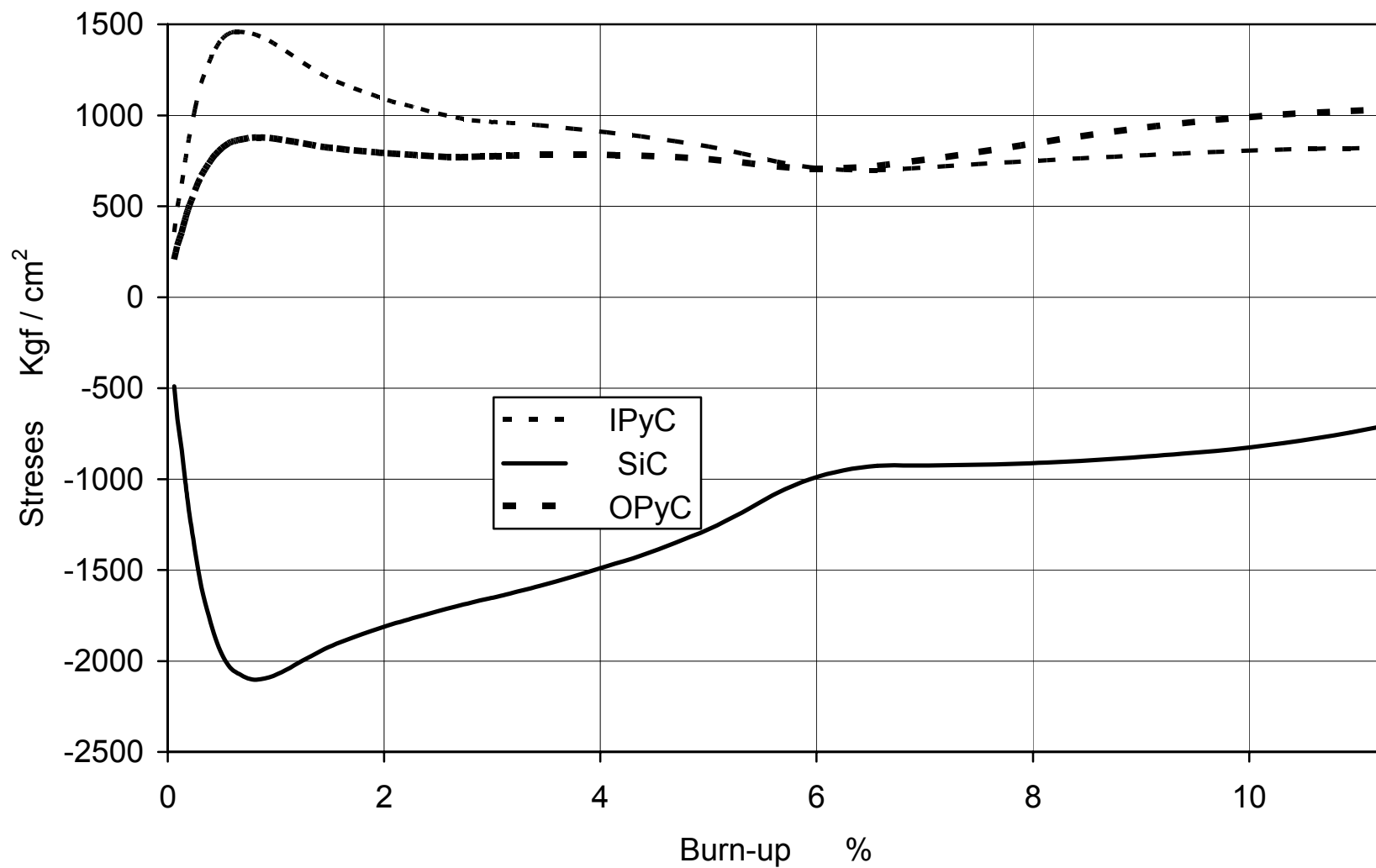


Fig. 1: Stresses in HFR K3

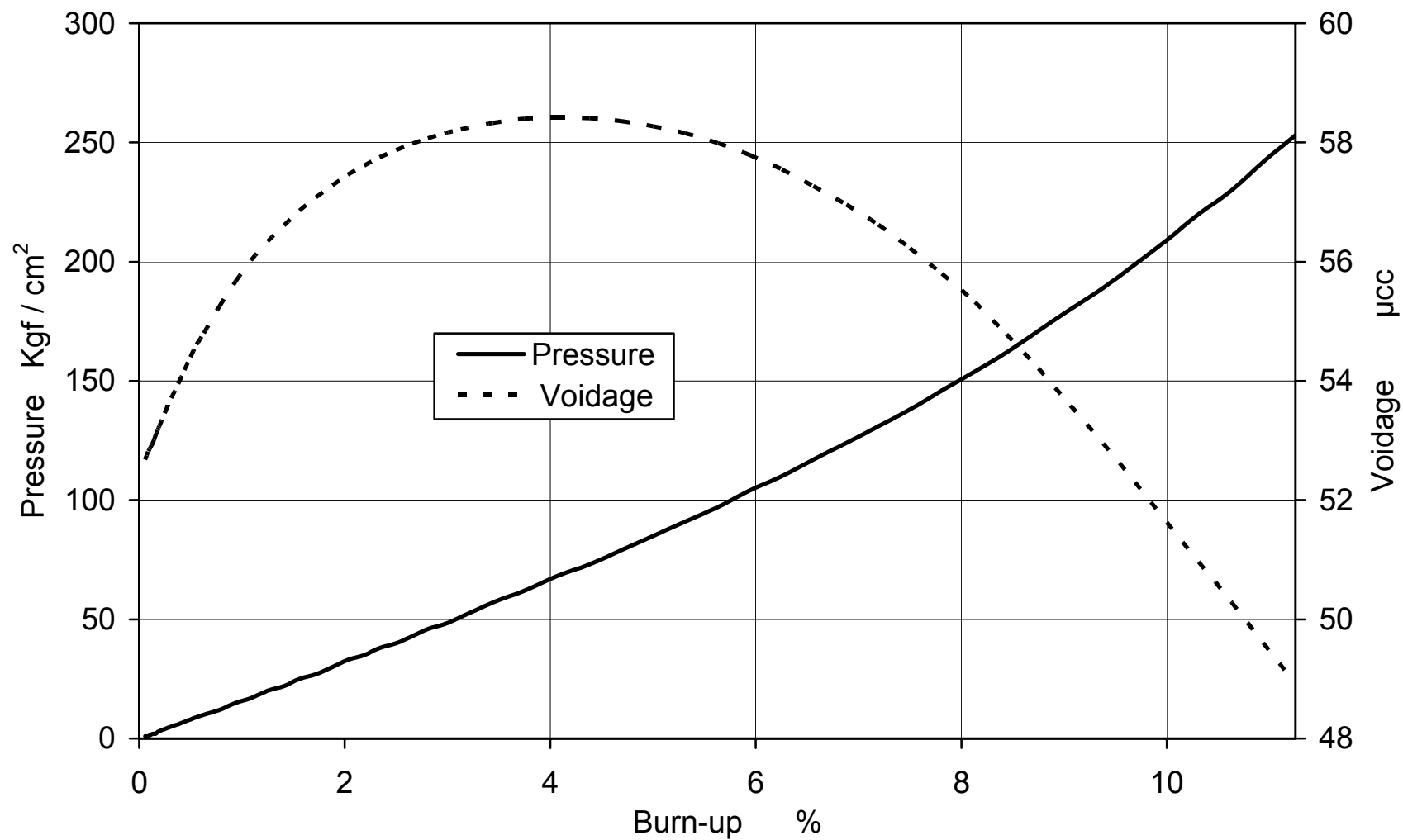


Fig.2 Gas Pressure and Voidage in HFR K3

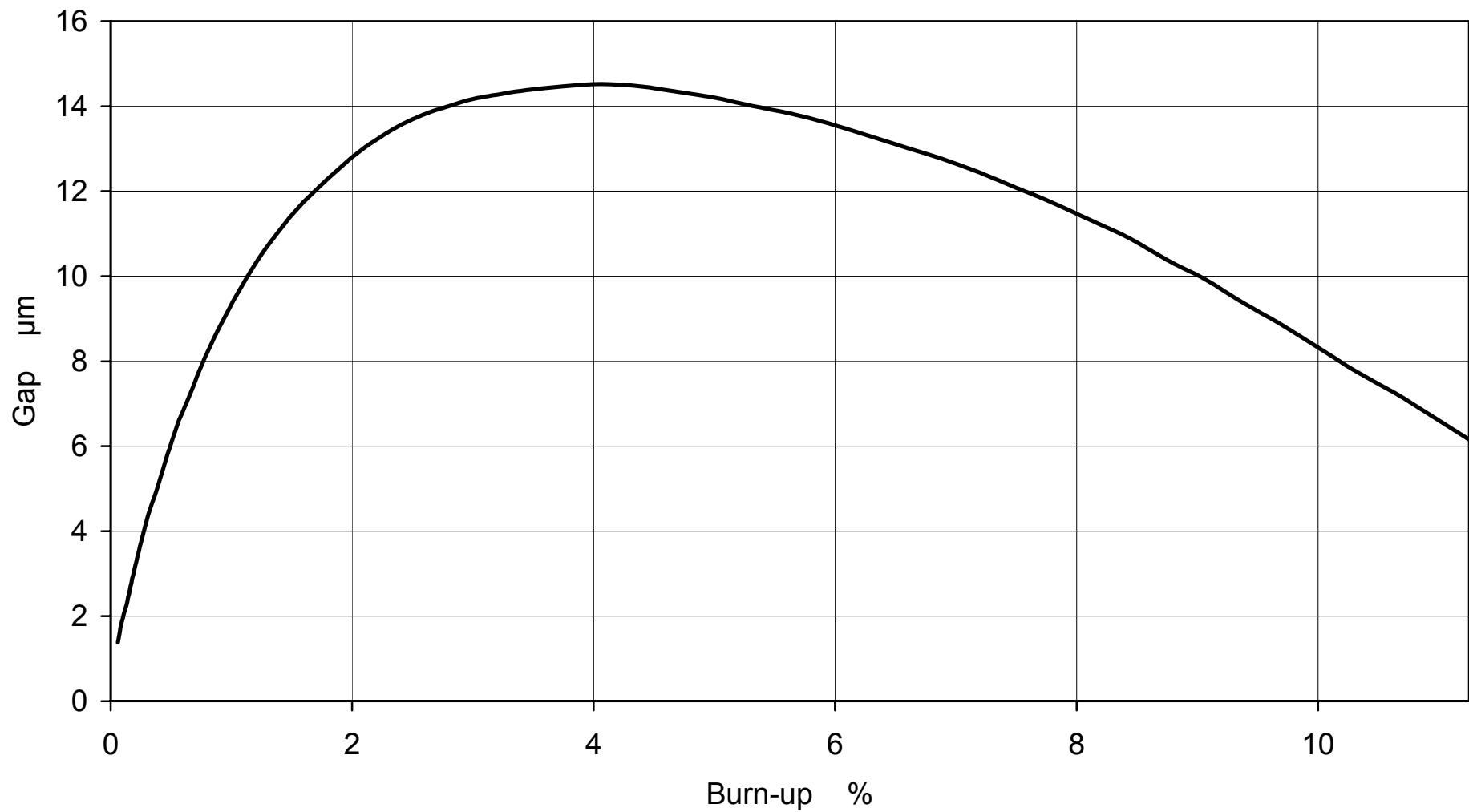


Fig.3: Kernel-Coating Radial Gap in HFR K3

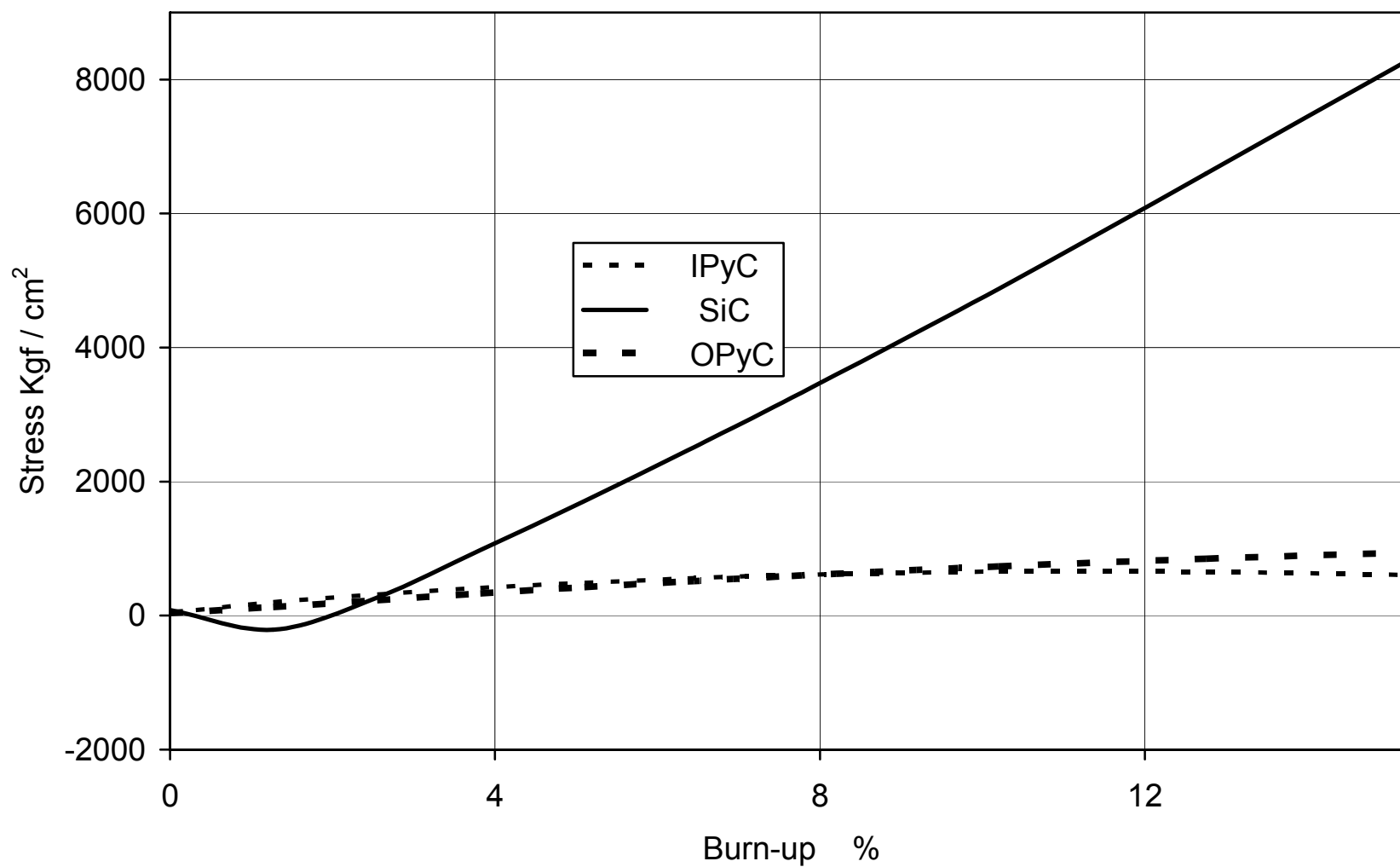


Fig. 4: Stresses in FRJ2 K15

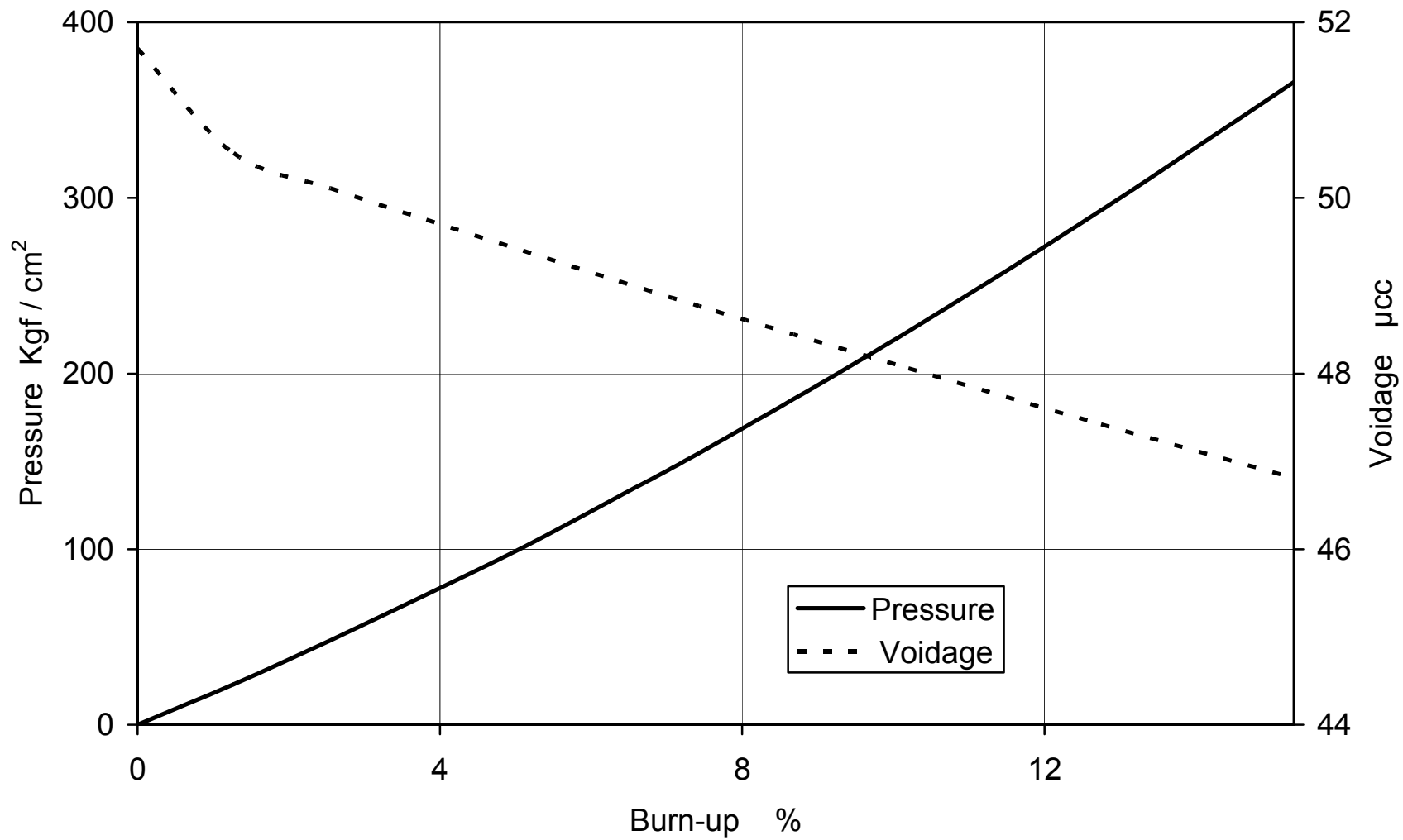


Fig.5: Gas Pressure and Voidage in FRJ2 K15

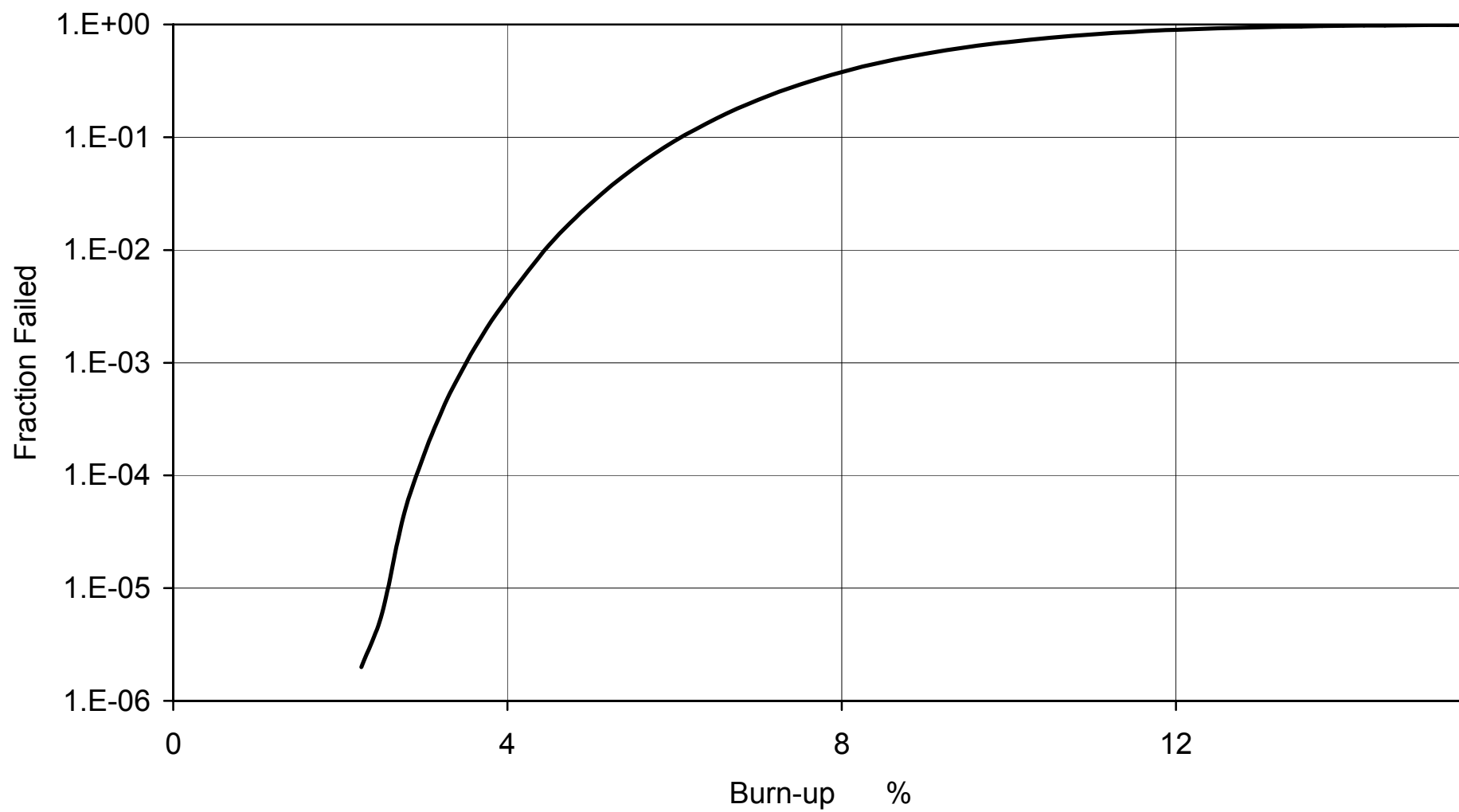


Fig.6: Failure Fractions in FRJ2 K15



FRAMATOME ANP

10, Rue Juliette Récamier
69456 LYON CEDEX 06
FRANCE

NUCLEAR FUEL

DESIGN AND SALES DIVISION

Type of document : Note d'étude, de calcul,
d'analyse, de synthèse, de
méthode

Class

N

Pages : 12


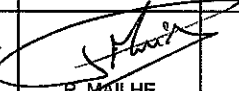
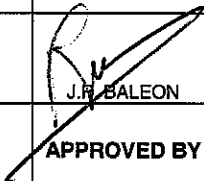
Appendices : 0

Document title

A BENCHMARK MODELLING OF IRRADIATION FRJ2-K15 BY ATLAS CODE

KEY-WORDS : - IRRADIATION - FRJ2 K15 - MODELLING - FAILURE - PARTICLE

Distribution	FFTC	FFTT (N. VIOUJARD)	FFTM (P. GUILLERMIER)	CEA DEC (M. PHELIPE)			
Purpose of distribution	GED Patrimoine	Pour info	Pour info	Diffus. Client			
Number	.pdf	.pdf	.pdf	.pdf			

A	08/11/2004	 L. DANIEL	 P. MAILHE		BPE	 J.R. BALEON
REV	DATE	AUTHOR	VERIFIED BY	MODIFICATIONS – COMMENTS	STATUS	APPROVED BY

CLASSIFICATION :

U.D. : 154701

INTERNAL IDENTIFICATION NUMBER

FFDC01494

This document is the property of FRAMATOME ANP SAS . No information contained herein may be divulged to a third party without the prior written approval of FRAMATOME ANP NUCLEAR FUEL – Design and Sales Division, under the terms of french law n° 57298 dated 11.03.1957.

REVISIONS

DATE	INDEX	OBSERVATIONS
08/11/2004	A	First issue

CONTENTS

- 1. INTRODUCTION 4
- 2. INPUT DATA AND IRRADIATION CONDITIONS 4
- 3. MODELLING HYPOTHESES 4
- 4. RESULTS 5
- 4.1 Run 1: CEA-CEGA models 5
- 4.2 Run 2: CEA-simplified models 6
- 5. CONCLUSION 6
- 6. REFERENCES 7

LIST OF TABLES

Table 1:	FRJ2-K15 fuel particle dimensions.....	8
Table 2:	FRJ2-K15 fuel particle characteristics.....	8
Table 3:	FRJ2-K15 irradiation conditions	9
Table 4:	Listing of pertinent data at different time steps – Run 1 CEA-CEGA models.....	9
Table 5:	Listing of pertinent data at different time steps – Run 2 CEA-simplified models, $T_{\text{gas}} = 1223\text{K}$	10
Table 6:	Listing of pertinent data at different time steps – Run 2 CEA-simplified models, $T_{\text{gas}} = 1323\text{K}$	10

LIST OF FIGURES

Figure 1:	Internal tangential stresses in IPyC, SiC and OPyC layers – Run 1 CEA-CEGA models..	11
Figure 2:	Internal tangential stresses in SiC for end-of-life fluence from 0.2E+25 to 2E+25 n/m ² - Run 1 CEA-CEGA models	11
Figure 3:	Internal tangential stresses in IPyC, SiC and OPyC layers with a gas temperature of 1223K – Run 2 CEA-simplified models	12
Figure 4:	Internal tangential stresses in IPyC, SiC and OPyC layers with a gas temperature of 1323K – Run 2 CEA-simplified models	12

1. INTRODUCTION

This study presents the results obtained with ATLAS V1.0 [1] by Framatome ANP for FRJ2-K15 irradiation.

The FRJ2-K15 experiment was irradiated 590 effective full power days.

The particularity of this irradiation is that the ratio fast neutron dose on burn-up is very low.

2. INPUT DATA AND IRRADIATION CONDITIONS

Tables 1 and 2 list dimensional and fuel characteristics. Particle dimensions are the typical German ones.

Table 3 lists irradiation conditions.

Calculations are made with two different average gas temperatures: 1223 and 1323 K in order to determine the influence of this parameter on results.

3. MODELLING HYPOTHESES

For all runs, the kernel laws are issued from UO₂ PWR experience by CEA.

For the two calculations carried out:

- In the first run, the buffer, the IPyC and OPyC layers are characterized with the CEGA model and the SiC layer with the CEA model, named CEA-CEGA.

In this case, the properties for buffer and PyC layers come from CEGA literature. Laws or constants are generally given as a function of the following parameters: fast fluence, temperature, degree of anisotropy, density and crystallite size, as appropriate.

For buffer, the Young's modulus is given by the following equation:

$$E = 34500 \cdot \exp(-2.03 \cdot P) \quad (P = \text{porosity, \%})$$

- In the second run, the buffer is described by a simplified model, IPyC and OPyC layers are described by the CEGA model and SiC layer is described by CEA model, named CEA-simplified.

In the simplified model, the buffer thermal characteristics are correctly represented. However, the mechanical characteristics are modified so that the buffer has no mechanical influence on the particle. Young's modulus is taken as very low and the irradiation induced dimensional change is not taken into account.

$$E = 10 \text{ MPa}$$

Actually, the buffer, by very rapidly irradiation induced dimensional change, failed, and no longer has any mechanical action on external layers [2].

The temperature defined in the input file read by ATLAS is the outside temperature on the OPyC layer whereas that given in the parameters of irradiation is the temperature of the gas. Whatever type of fuel is studied (pebble or compact) the particle is inserted into a graphite matrix. To take into account the thermal conductivity in a pebble (or a compact), the gradient temperature has been over estimated by 200°C.

$$T_{OPyC}^{ext} = T_{gas} + 200$$

4. RESULTS

4.1 Run 1: CEA-CEGA models

CEA-CEGA models, with a end-of-life fluence of 0.2E+25 n/m² and an average gas temperature of 1223K, seem not describe reality (see figure 1). The evolution of internal tangential stresses in SiC, observed with such hypotheses, doesn't represent the realistic stress history. With CEA-CEGA models, the buffer is considered sufficiently rigid to have a mechanical interaction with the others coatings. It explains the high values of tangential stresses in SiC layer.

With such stress history in SiC, at the end of irradiation, the number of failed particles is higher than the admitted value (see table 4).

Experimentally, the particle failure fraction is considered lower than 10⁻⁵ [3].

By using CEA-CEGA models for buffer with a end-of-life fluence of 0.2E+25 n/m², modelling and experiment are not in agreement.

In a second step, the end-of-life fluence has been increased with a constant end-of-life burn-up, in order to determine the limit of CEA-CEGA models.

On the figure 2, are presented the internal tangential stresses calculated with different values for end-of-life fluence. It varies from 0.2E+25 n/m² to 2E+25 n/m².

It appears that for end-of life fluence greater than 0.6E+25 n/m², the internal tangential stresses evolution in SiC is the typical one.

Figure 2 underlines the limit of the CEA-CEGA models: it seems not describe reality for fluence less than 0.6E+25 n/m².

These non-awaited results can be explained by mechanical hypotheses used and are not depending on gas temperature. It's why only one calculation has been made with a gas temperature of 1223K.

4.2 Run 2: CEA-simplified models

Two calculations have been made with two gas temperatures: 1223 and 1323K in order to study the influence of this parameter on results.

Using CEA-simplified models for buffer, evolution of tangential stress history appears as awaited. The buffer is defined in order to have no mechanical interaction with the others layers. It follows the displacements of the kernel and the IPyC layer. It explains that the tangential stresses in SiC layer are lower than in the first run.

Difference for minimal tangential stresses in SiC between 1223 and 1323K can be noticed and explained by the fact that the internal pressure increases with temperature.

Irradiation induces creep in the pyrocarbon layers which tends to relax the stresses and equilibrium is established between densification and relaxation. Pressure counters PyC shrinkage and the stresses on the layers change:

- The compression stress in the SiC decreases in absolute values. At the end of irradiation, whatever the models used, the SiC is under compression.
- The tensile stress in the IPyC decreases.

Higher the temperature is, faster the internal pressure increases and faster the compression strain in the SiC decreases in absolute values (see figures 3 and 4, and tables 5 and 6).

Whatever the gas temperature used, the SiC layer is always under compression during irradiation duration.

The particle failure fraction during irradiation is determined by the Weibull's law. The SiC layer being under compression, there is no failure fraction with such hypotheses, which better corresponds to the results from experiment.

5. CONCLUSION

The FRJ2-K15 irradiation is a non-conventional irradiation because of a very low ratio fast neutron dose on burn-up.

Two main calculations have been made.

- For the first run, the buffer is described by CEA-CEGA models.

With a fluence of $0.2E+25$ n/m², the number of failed particles is higher than the admitted value.

It seems that there is a limit to the CEA-CEGA models because stress history in SiC doesn't match the awaited evolution for fluence less than $0.6E+25$ n/m².

- For the second run, the buffer is described by a simplified model so that it has no mechanical influence on the particle. With such hypothesis, no particle failure fraction is observed on this point. Modelling and experiments seem to be in good agreement.

It appears that results are strongly dependent on modelling of the buffer. The knowledge about the behaviour of this layer is quite poor, whereas it appears to be an important parameter for the particle modelling.

6. REFERENCES

- [1] "Notice d'utilisation d'ATLAS V1.0" – Technical document SESC/LSC 03-040 – F. MICHEL – October 2003
- [2] HTR-F Project – "Deliverable 13 ATLAS First calculations" – Technical document SESC/LIAC 03-019 – G. DEGENEVE – October 2003
- [3] "A benchmark modelling of irradiations in HFR-K3 and FRJ2-K15" - D. G. MARTIN, consultant to British Nuclear Fuels plc – June 2004

Table 1: FRJ2-K15 fuel particle dimensions

Parameter	Units	Value
Kernel diameter	μm	501 ± 10.8
Buffer thickness	μm	92 ± 14.3
IPyC thickness	μm	38 ± 3.4
SiC thickness	μm	33 ± 1.9
OPyC thickness	μm	41 ± 3.8

Table 2: FRJ2-K15 fuel particle characteristics

Parameter	Units	Value
Oxygen to Uranium ratio	Atom ratio	2
Carbon to Uranium ratio	Atom ratio	0
U-235 enrichment	Weight %	16.76
IPyC density	-	~1.9
SiC density	-	3.2
OPyC density	-	1.88
IPyC BAF	-	1.029
OPyC BAF	-	1.020

BAF = Bacon Anisotropy Factor

Table 3: FRJ2-K15 irradiation conditions

Parameter	Units	Value
Irradiation duration	efpd	590
End of life burn-up	% FIMA	15.3
End of life fluence	E+25 n/m ² E>0.18MeV	0.2
Average gas temperature	K	1223 and 1323
Ambient gauge pressure	MPa	0.1

Table 4: Listing of pertinent data at different time steps – Run 1 CEA-CEGA models

EFPD (d)	0	1	10	51	100	202	401	590
BurnUp (%FIMA)	0.00%	0.03%	0.26%	1.33%	2.60%	5.23%	10.40%	15.30%
BurnUp (MWd/tHM)	0	298	2 428	12 516	24 439	49 200	97 806	143 844
Fluence (E+25 n/m ²)	0.0000	0.0004	0.0034	0.0174	0.0340	0.0687	0.1361	0.1999
Particle power (W)	0.00	0.15	0.15	0.15	0.15	0.15	0.15	0.15
T kernel center (°C)	1700	1270	1270	1267	1268	1268	1269	1270
T external particle (°C)	1700	1250	1250	1250	1250	1250	1250	1250
Internal pressure (bars)	1	1	1	4	20	83	244	440
σ_{θ} IPyC (inner) (MPa)	0	-2	-1	19	32	47	67	75
σ_{θ} IPyC (outer) (MPa)	0	-2	0	14	23	36	51	56
Radial densification IPyC	0.0%	0.0%	0.0%	0.0%	0.0%	-0.1%	-0.2%	-0.2%
Tangential densification IPyC	0.0%	0.0%	0.0%	0.0%	-0.1%	-0.1%	-0.2%	-0.3%
σ_{θ} SiC (inner) (MPa)	0	6	1	153	221	284	400	522
σ_{θ} SiC (outer) (MPa)	0	5	1	139	201	259	364	475
σ_{θ} OPyC (inner) (MPa)	0	-2	-1	21	35	55	85	106
σ_{θ} OPyC (outer) (MPa)	0	-2	0	19	32	50	78	97
Particle failure fraction	0	0	0	8.6E-7	1.6E-5	1.3E-4	2.1E-3	1.8E-2

Table 5: Listing of pertinent data at different time steps – Run 2 CEA-simplified models,
 $T_{\text{gas}} = 1223\text{K}$

EFPD (d)	0	1	10	51	100	202	401	590
BurnUp (%FIMA)	0.00%	0.03%	0.26%	1.33%	2.60%	5.23%	10.40%	15.30%
BurnUp (MWd/tHM)	0	298	2 428	12 516	24 439	49 200	97 806	143 844
Fluence (E+25 n/m ²)	0.0000	0.0004	0.0034	0.0174	0.0340	0.0687	0.1361	0.1999
Particle power (W)	0.00	0.15	0.15	0.15	0.15	0.15	0.15	0.15
T kernel center (°C)	1600	1188	1190	1186	1187	1187	1188	1188
T external particle (°C)	1600	1150	1150	1150	1150	1150	1150	1150
Internal pressure (bars)	1.0	0.8	1.0	1.9	5.6	40.3	142.6	262.1
σ_{θ} IPyC (inner) (MPa)	0	-1	0	9	18	37	69	94
σ_{θ} IPyC (outer) (MPa)	0	-1	0	8	17	34	63	84
Radial densification IPyC	0.00%	0.00%	0.00%	-0.02%	-0.04%	-0.09%	-0.17%	-0.25%
Tangential densification IPyC	0.00%	0.00%	0.00%	-0.03%	-0.05%	-0.10%	-0.19%	-0.28%
σ_{θ} SiC (inner) (MPa)	0	3	-1	-18	-37	-60	-80	-76
σ_{θ} SiC (outer) (MPa)	0	2	-1	-17	-34	-55	-74	-70
σ_{θ} OPyC (inner) (MPa)	0	-1	0	7	15	30	57	78
σ_{θ} OPyC (outer) (MPa)	0	-1	0	7	14	28	52	71

Table 6: Listing of pertinent data at different time steps – Run 2 CEA-simplified models,
 $T_{\text{gas}} = 1323\text{K}$

EFPD (d)	0	1	10	51	100	202	401	590
BurnUp (%FIMA)	0.0%	0.0%	0.3%	1.3%	2.6%	5.2%	10.4%	15.3%
BurnUp (MWd/tHM)	0	298	2 428	12 516	24 439	49 200	97 806	143 844
Fluence (E+25 n/m ²)	0.000	0.000	0.003	0.017	0.034	0.069	0.136	0.200
Particle power (W)	0.00	0.15	0.15	0.15	0.15	0.15	0.15	0.15
T kernel center (°C)	1600	1288	1287	1287	1287	1287	1287	1288
T external particle (°C)	1600	1250	1250	1250	1250	1250	1250	1250
Internal pressure (bars)	1	1	1	4	19	70	203	364
σ_{θ} IPyC (inner) (MPa)	0	-2	0	9	19	38	69	92
σ_{θ} IPyC (outer) (MPa)	0	-2	0	8	17	34	62	82
Radial densification IPyC	0.00%	0.00%	0.00%	-0.02%	-0.04%	-0.08%	-0.17%	-0.24%
Tangential densification IPyC	0.00%	0.00%	-0.01%	-0.03%	-0.05%	-0.10%	-0.20%	-0.30%
σ_{θ} SiC (inner) (MPa)	0	3	-1	-17	-31	-48	-53	-26
σ_{θ} SiC (outer) (MPa)	0	3	0	-16	-29	-45	-49	-25
σ_{θ} OPyC (inner) (MPa)	0	-2	0	7	15	32	58	79
σ_{θ} OPyC (outer) (MPa)	0	-1	0	7	14	29	54	72

Figure 1: Internal tangential stresses in IPyC, SiC and OPyC layers – Run 1 CEA-CEGA models

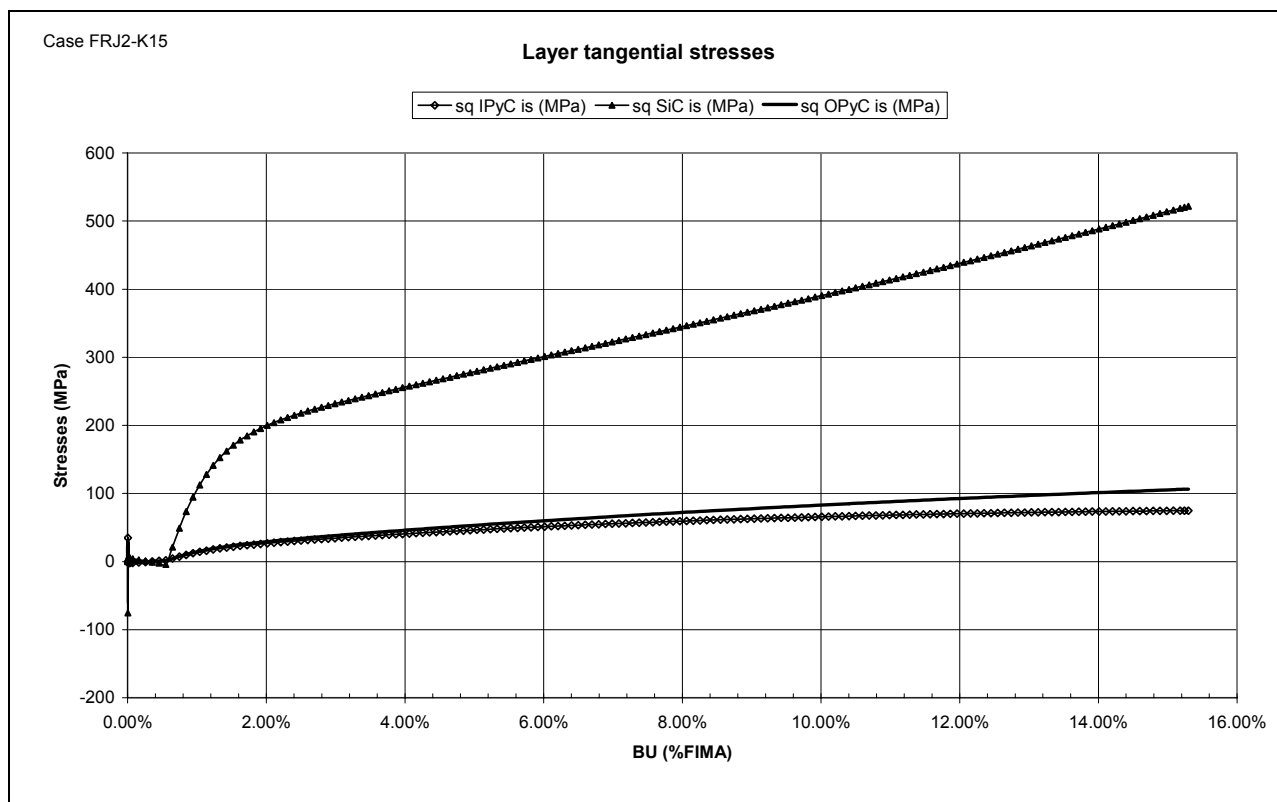


Figure 2: Internal tangential stresses in SiC for end-of-life fluence from $0.2E+25$ to $2E+25$ n/m^2 - Run 1 CEA-CEGA models

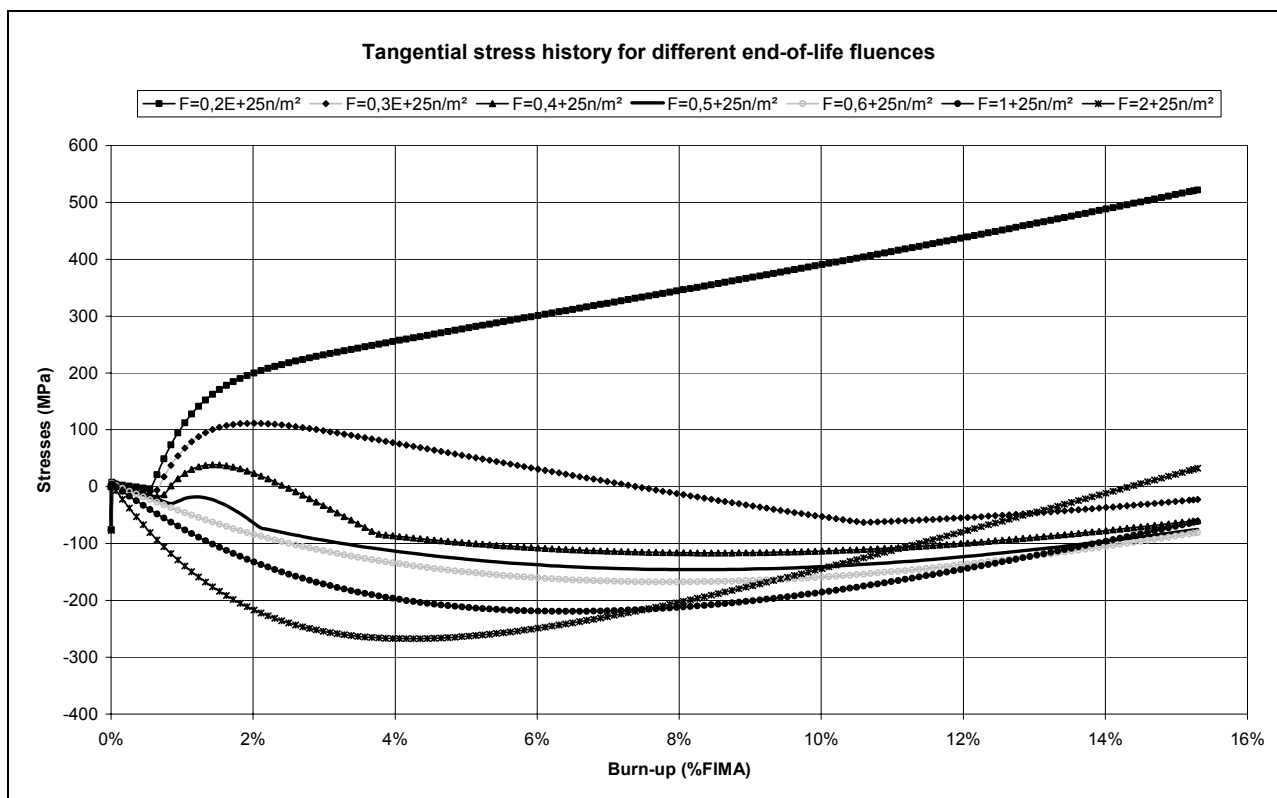


Figure 3: Internal tangential stresses in IPyC, SiC and OPyC layers with a gas temperature of 1223K – Run 2 CEA-simplified models

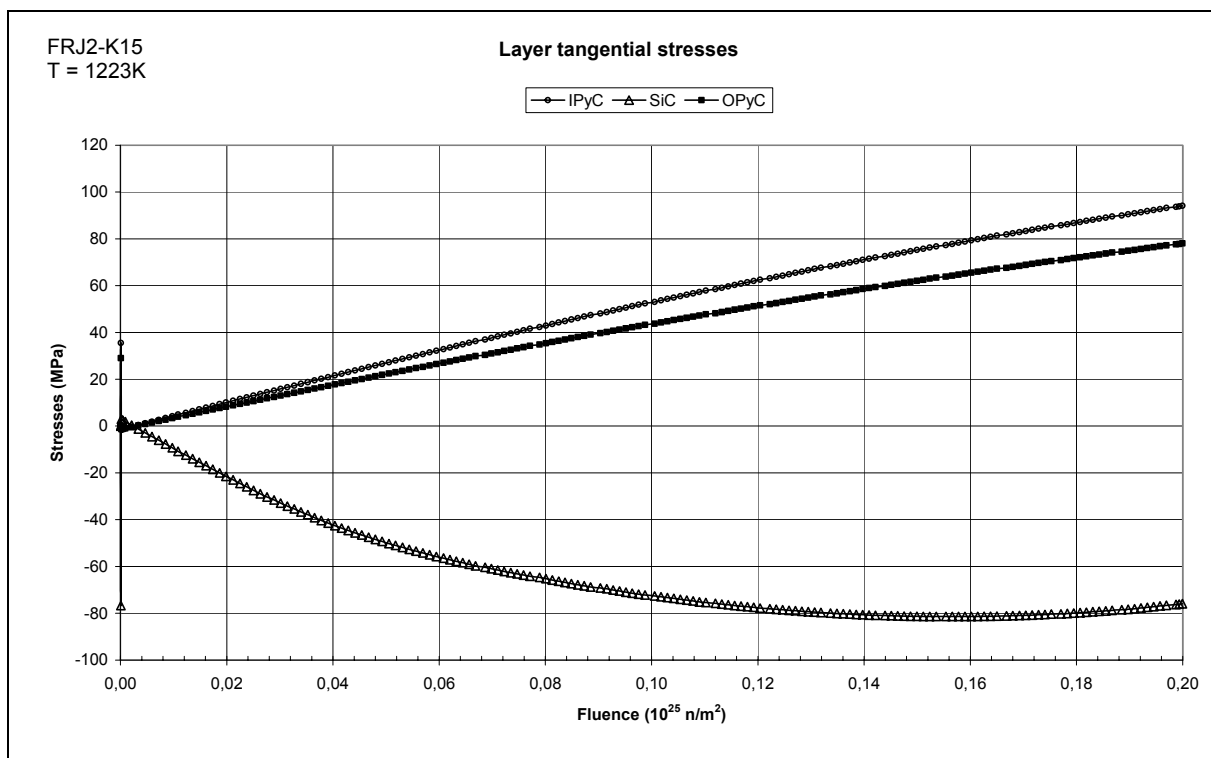
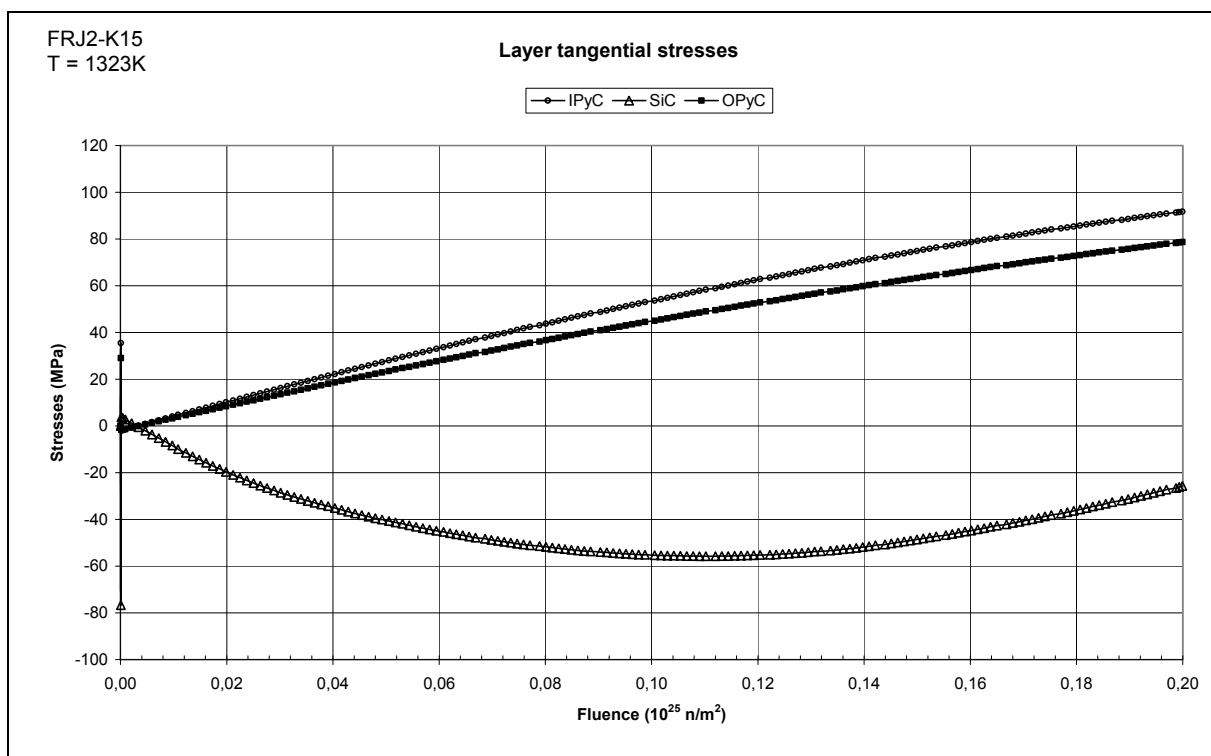


Figure 4: Internal tangential stresses in IPyC, SiC and OPyC layers with a gas temperature of 1323K – Run 2 CEA-simplified models





DIRECTION DE L'ÉNERGIE NUCLÉAIRE

DIRECTION DU CEA/CADARACHE

DÉPARTEMENT D'ÉTUDES DES COMBUSTIBLES

SERVICE D'ÉTUDES ET DE SIMULATION DU COMPORTEMENT DES COMBUSTIBLES

LABORATOIRE DE CONCEPTION ET D'IRRADIATIONS DE COMBUSTIBLES INNOVANTS

HTR-F1 PROJECT - CONTRIBUTION TO DELIVERABLE N°3.3
HFR-K3 CALCULATION WITH ATLAS CODE

DE M. PHÉLIP, G.DEGENÈVE

Note Technique SESC/LC2I 04-022

Indice 0

de décembre 2004

Note Technique SESC/LC2I 04-022

Indice 0

Page 1/23

Titre : HTR-F1 PROJECT - CONTRIBUTION TO DELIVERABLE N°3.3
HFR-K3 CALCULATION WITH ATLAS CODE

Auteur(s) : M. PHÉLIP, G.DEGENÈVE

Résumé :

This document is the CEA contribution of the deliverable n°3.3 of the HTR-F1 project, Work-Package 3, Fuel Modeling. Its purpose is to present the calculations of the HFR-K3 experiment performed with the ATLAS code, to be compared with STRESS3 and CONVOL.

Because PyC irradiation induced dimensional change and creep constant are very important parameters, three calculations with the three set of PyC data selected in the framework of the project have been performed for each pebble.

With the FZJ and BNFL PyC data, the SiC layer of the particle in its nominal geometry is never in tension, leading to zero failure during irradiation.

With the CEGA PyC data, the SiC layer of the particle is in tension at EOL for the HFR-K3/3 pebble and a simple statistical analysis leads to less than one failed particle. While taking CEGA properties is not justified because these properties are more adapted to US particles than to German's, this failure value is not inconsistent with the irradiation results.

Mots Clés

HFR-K3 - ATLAS - HTR - PYC - BENCHMARK

N° EOTP

A-SCRCG-09

En l'absence d'accord ou de contrat, les informations contenues dans le présent document ne sont pas destinées à la publication, il ne peut en être fait état sans autorisation expresse du Chef de Service.

	Nom	Visa	Date	Classification				
Assurance Qualité	G. ARÈNE			Lib	DR	CC	CD	SD
Approbateur	F. SUDREAU			X				
Vérificateur	M. PELLETIER			Cadre de réalisation du document				
Rédacteur	M. PHÉLIP			DPSF/SFS				



REVISIONS

DATE	OBSERVATIONS	INDEX
Dec. 2004	First issue	0



CONTENTS

1. INTRODUCTION	4
2. BASIC DATA	4
2.1. GENERAL POINTS	4
2.2. PHYSICAL AND MECHANICAL PROPERTIES OF MATERIALS	5
2.2.1. Kernel	5
2.2.2. Layers	5
2.3. LOADINGS	6
2.3.1. Thermal calculation	6
2.3.2. Mechanical calculation	7
3. CALCULATIONS	7
3.1. MODELING	7
3.2. CALCULATIONS	8
3.3. RESULT ANALYSIS	9
3.3.1. Thermal calculations	9
3.3.2. Mechanical calculations	9
4. CONCLUSIONS	10
REFERENCES	11
LIST OF TABLES	12
LIST OF FIGURES	14
LIST OF ANNEXES	22

1. INTRODUCTION

This document is the CEA contribution of the deliverable n°3.3 of the HTR-F1 project, Work-Package 3, Fuel Modeling. Its purpose is to present the calculations of the HFR-K3 experiment performed with the ATLAS code [1], under development at the CEA/DEN/DEC/SESC/LSC.

It presents a deterministic thermal and mechanical calculation on a single particle using the ATLAS code in its V1.0 version. In addition, a simple statistical study gives a failure fraction estimation to be compared with the results of the experiment.

2. BASIC DATA

2.1. GENERAL POINTS

The HFR-K3 experiment was irradiated 359 EPFD in HFR, from 04/15/82 to 09/05/83. The objective of HFR-K3 was to test the integral performance of fuel elements containing UO₂ LTI Triso particles from the LEU Phase 1 coating batch EUO 2308, a pre-runner of the large scale AVR 19 GLE-3 production with 24,600 spheres particles. The fabrication and irradiation data are coming from [2].

The data on the particles are gathered in the following table :

Test	HFR-K3
Coated particle batch	EUO 2308
Kernel composition	LEU UO ₂
Enrichment [U-235 wt.%]	9.82
Kernel diameter [μm]	497 \pm 14.1
Buffer layer thickness [μm]	94 \pm 10.3
IPyC layer thickness [μm]	41 \pm 4.0
SiC layer thickness [μm]	36 \pm 1.7
OPyC layer thickness [μm]	40 \pm 2.2
Kernel density [g/cm ³]	10.81
Buffer density [g/cm ³]	1.00
IPyC density [g/cm ³]	~ 1.9
SiC density [g/cm ³]	3.20
OPyC density [g/cm ³]	1.88
IPyC Anisotropy [BAF]	1.053
OPyC Anisotropy [BAF]	1.019

Four fuel spheres were irradiated. The rig contained three irradiation capsules and the fuel spheres were arranged one to a capsule for both the top and bottom capsules and with two fuel spheres in the medial capsule (see figure 1). An X-rays picture of the top capsule is shown on figure 2. The capsules HFR-K3/1 (top position) and HFR-K3/3 (medial position) have been selected for benchmarking [2].

The main irradiation data are :

Pebble	HFR-K3/1	HFR-K3/3
Irradiation time (EPFD)	359	359
Peak burn-up (%FIMA)	7.5	10.6
Peak fluence(10^{25} n/m ² E>16fJ)	4.0	5.9
Pebble centre temperature (°C)	1200	920

The irradiation results, coming from [2] are given table 1. The level of in-pile ^{85m}Kr R/B measurements at beginning of life (BOL) and at end of life (EOL) showed that there was no manufacturing defect and no additional failures during the irradiation (the low value of R/B corresponds to the fissions of the Uranium free in the matrix).

2.2. PHYSICAL AND MECHANICAL PROPERTIES OF MATERIALS

2.2.1. Kernel

The kernels are made of low enriched UO₂ and were fabricated with the SOL-GEL process. The properties used for the modeling are those taken from document [3] defined within the 5th FWP HTR-F project. The properties used are density ρ , thermal conductivity λ (first law), coefficient of thermal expansion α , Young's modulus E and the Poisson ratio ν . The fuel creep (thermal and irradiation) is not taken into account at this stage.

The total porosity of the kernel is deduced from the theoretical density given in the note Ref. [3] and the fabrication density of the kernel (10.81) given in §2.1 : $p = (10.95 - \rho)/10.95 = 0.0128$ (1.28%)

2.2.2. Layers

The properties which are used for the buffer, the PyC and SiC dense layers are thermal conductivity λ , the coefficient of thermal expansion α , the Young's modulus E, the Poisson's ratio ν and the irradiation induced creep law. Several calculation cases with different values for these properties were studied (see § 3.2). The values taken into account come from the note Ref [3]. More particularly, the « BNFL » and « FZJ » data are those proposed by these organizations within the framework of the European HTR-F contract.

The porosity of the layers is deduced from the theoretical density of pyrocarbon and of SiC given in Ref [3] and from the layer density given in §2.1 :

Layers	Theoretical density (g.cm ⁻³)	Measured density (g.cm ⁻³)	Fabrication porosity (%)
Buffer	2.27	1.00	55.9
IPyC	2.27	1.86	17.2
SiC	3.238	3.20	1.2
OPyC	2.27	1.88	17.2

2.3. LOADINGS

2.3.1. Thermal calculation

The thermal loading has two components :

- The power released by fission in the kernel. In the ATLAS application, this value is calculated using the number of fissions per second and per fuel volume unit, which is an input data, theoretically dependent on time. This last value is not provided in the note [2]. It is re-calculated using known data, namely burnup and irradiation time. This re-calculated value is thus an average value over the length of the irradiation. This assumption is a simplifying one, in the absence of a simplified neutronic modulus which could take into account the depletion in ²³⁵U and the enrichment in ²³⁹Pu and other fissile isotopes.

$$BU = 100.(\tau.t.M_{HM})/(N_a.\rho_{HM}.10^3) \quad \text{and} \quad P = 10^6.E.e.\tau \quad \text{with :}$$

BU	burn-up fraction	(%FIMA)
τ	fission rate	(fissions.m ⁻³ .s ⁻¹)
t	time	(s)
M_{HM}	molar atom weight	(g)
N_a	Avogadro number	(6.0221.10 ²³)
ρ_{HM}	heavy metal density	(kg.m ⁻³)
P	volumic power	(W.m ⁻³)
E	mean value of fission energy	(E = 200 MeV)
e	conversion J/eV	(1.602.10 ⁻¹⁹)

Pebble	K3/1	K3/3
Time averaged fission rate (fissions.m ⁻³ .s ⁻¹)	5.91.10 ¹⁹	8.35.10 ¹⁹
Time averaged power per particle (W)	0.16	0.23

- The imposed temperature to the model. This is the temperature of the external surface of the external PyC layer. By simplification, this temperature is taken as equal to the pebble centre temperature (see §2.1).

2.3.2. Mechanical calculation

The loads of the mechanical calculations are of imposed pressure or deformation type and result from the following physical phenomena :

- *Release from the kernel of fission gases Xe and Kr and production of CO* (formed with the buffer carbon and the oxygen released after the fission of a Uranium atom or of a Plutonium atom). These gases generate a pressure which is applied to the inner wall of the IPyC layer and on the external wall of the kernel. This pressure both depends on the quantity of gas and the size of the free volume. The free volume as well as the quantity of gas formed, then released, are calculation results (see §3.1).

The value chosen for the production of stable Xe and Kr is of 0.301 atom of gas formed for one split atom. Only a part of the gas formed is released. The release model used is given in Ref.[3], §3.3.3, CEA model 2. This model, such as used in ATLAS, was simplified: an abacus function of the temperature and the burnup by considering a burnup to constant irradiation time ratio gives, at each step of the irradiation, the FG release.

The CO production law is given in Ref [3], §3.4.2, PROKSCH model. This law is valid for low enriched UO₂ fuels.

- *Influence of the graphite matrix of the compact on the particle.* This influence is for the time being, taken into account by a pressure applied on the external OPyC layer. In a first stage, this pressure is taken as equal to 0.1 MPa.

- *Fuel swelling of the kernel.* This includes the solid and gaseous swellings. The solid and gaseous swelling laws are given in Ref [3].

- *Fuel densification.* The densification law is given in Ref. [3]. Due to the low level of porosity, this model is not started up.

- *PyC and SiC layer irradiation induced dimensional change rate.* The laws are given in Ref. [3]. These laws are expressed versus the fast fluence. The fast flux not being provided in [2], the latter is taken as constant during the irradiation and as equal to the total fluence divided by the irradiation time.

Capsule	1	3
Fast flux (10^{25} n.m ⁻² .s ⁻¹ E>16fJ)	$1.29.10^{18}$	$1.90.10^{18}$

3. CALCULATIONS

3.1. MODELING

The modeling is detailed in Ref [1]. It is briefly described below.

A finite element method is used and is followed by :

- A thermal calculation giving the temperature field in the meshing nodes.
- A mechanical calculation allows access to the displacements fields, stresses and strains in the meshing nodes. The particle model is a two-dimensional modeling and represents a slice of the particle.

The main characteristics of the model are as follows:

- The thermal load is the temperature field resulting from the thermal calculation.
- The pressure load is calculated at each time step from the free volume (itself calculated from the deformed geometry), the temperature and the quantity of gas (Xe, Kr, CO) present.
- The swelling of the kernel and the irradiation induced deformation of the layers are considered as loads of imposed deformation type. These are taken into account by making an analogy between swelling and thermal expansion.

3.2. CALCULATIONS

The first ATLAS calculations [4] showing that the results were highly dependant on the properties taking into account, parametric calculations with various PyC properties are proposed:

Calculated cases	Properties		
	Buffer	PyC	SiC
HFR-K3/1	(1) Thermal properties are taking into account but mechanical properties are specific : no irradiation induced dimensional change rate and very low Young modulus	CEGA	CEA
HFR-K3/1		BNFL	
HFR-K3/1		FZJ	
HFR-K3/3		CEGA	
HFR-K3/3		BNFL	
HFR-K3/3		FZJ	

(1) : the buffer thermal characteristics are correctly represented. However, the mechanical characteristics are modified so that the buffer has no mechanical influence on the particle. Young's modulus is taken as very low (10 MPa) and the irradiation induced dimensional change is not taken into account. Actually, the buffer, by very fast irradiation induced dimensional change, failed, and no longer has any mechanical action on the dense layers.

3.3. RESULT ANALYSIS

3.3.1. Thermal calculations

Figure 3 shows the evolution of temperatures in the kernel and in the layers versus burn-up for the two cases HFR-K3/1 and HFR-K3/3 and for the three sets of properties.

The ΔT in the gaseous gap between the buffer and the IPyC increases with irradiation progress, reaches a maximum and decreases at the end of irradiation in the two cases. This gaseous gap is created by the radial shrinkage of the IPyC. Because the IPyC is bonded to the SiC, the shrinkage direction is toward the SiC layer. In the three set of data, the radial irradiation induced dimensional change is a shrinkage at the beginning of the irradiation and becomes swelling at the end. The inversion of the radial dimensional change for the FZJ data appears earlier than for CEGA and BNFL. Therefore, at about 9.5 at% (HFR-K3/3), the gap between the buffer and the IPyC is closed again and the temperature of the inner skin of the IPyC is the same as outer skin of buffer.

The kernel centre temperature difference between the three calculations is less than 10°C.

3.3.2. Mechanical calculations

Figure 4 shows the evolution of tangential stresses in the layers versus burn-up for the two cases HFR-K3/1 and HFR-K3/3 and for the three sets of properties.

The irradiation induced dimensional change of the pyrocarbon layers is countered by the SiC layer, which is about 10 times more rigid. This pyrocarbon dimensional change quickly creates circumferential compression stresses in the SiC layer and tensile stresses in the pyrocarbon layers. The irradiation induced creep in the pyrocarbon layers tends to relax the stresses before the latter become too great and an equilibrium is created between densification and irradiation induced creep relaxation. This equilibrium is reached very early on during irradiation (between 1 and 2 at%, depending on the properties taking into account).

The irradiation induced dimensional change and the creep constant are independent from temperature in the BNFL and FZJ PyC properties (see [3]): the SiC extremum compressive stress is the same for the two cases, about -750 MPa for FZJ but only -250 MPa for BNFL. The differences in stresses between BNFL and FZJ are mainly due to the difference of creep coefficient [3][4]. In the other hand, the CEGA PyC properties are temperature (and anisotropy) dependant (see figure 6): it is not surprising to see that the SiC maximum compressive stress is not equal in the two cases, about -300 MPa at 1200°C for HFR-K3/1 and about -450 MPa at 920°C for HFR-K3/3. The stresses are greater at low temperature while the irradiation induced dimensional change is lower (see figure 6, dimensional change): the stress relaxation is nevertheless much more important at high temperature (see figure 6, creep factor).

Once the equilibrium is reached, the pressure in the particle free volume due to the release of fission gases and of the CO production increases and changes the stresses on the layers: the compression stress in the SiC layer starts decreasing (in absolute value). Figure 5 shows the evolution of pressure inside the particle versus burn-up for the two cases HFR-K3/1 and HFR-K3/3 and for the three sets of PyC

properties. In each case (K3/1 and K3/3), there is no significant difference between the sets of PyC properties because the total free volume is not very dependent of these properties.

In the two cases, the calculated pressure is the same at end of life (EOL), about 90 bars. The temperature effect (1200°C) on the released gaseous FP and the pressure in the case of HFR-K3/1 compensates the higher production of gaseous FP in the case of HFR-K3/3. To be sure of this effect, an additional case has been performed: same burn-up as HFR-K3/3, but the temperature is equal to HFR-K3/1's. In that case, the effect of temperature on pressure and on released fraction is cumulated to the higher burn-up. The pressure at EOL is 140 bars.

With the FZJ and BNFL PyC properties, the SiC layer is never in tension. For finding SiC layers in tension, the layer thickness distribution would have to be taken into account. A simple statistical analysis based on the distribution density of failure expressed in term of a two parameter Weibull equation

$$f = 1 - \exp\left\{-\ln 2\left(\frac{\sigma}{\sigma_{\text{med}}}\right)^m\right\}$$
 where σ_{med} and m are constants determined from experiments and σ the maximum tensile stress in the SiC layer is not possible.

In the case of HFR-K3/3, this simple analysis can be made with the CEGA PyC properties because the SiC layer is in tension at EOL (see figure 4). It has been made, to be consistent, with values of σ_{med} and m coming from CEGA ($\sigma_{\text{med}} = 406$ MPa and $m = 6$). This analysis is showed on figure 7: at EOL, the failure fraction is equal to $2.74 \cdot 10^{-5}$, that is to say, for two pebbles of 16400 particles each, less than one failed particle in the center capsule. While taking CEGA properties is not justified because these properties are more adapted to US particles than to German's, it leads to failure values which are not inconsistent with the irradiation results.

CONCLUSIONS

This document presented the calculations of two pebbles of the HFR-K3 experiment performed with the ATLAS code. The irradiation results showed that no particle failed during irradiation.

Because PyC irradiation induced dimensional change and creep constant are very important parameters, three calculations with the three set of PyC data selected in the framework of the project have been performed ("FZJ", "BNFL" and "CEGA") for each pebble.

With the FZJ and BNFL PyC data, the SiC layer of the particle **in its nominal geometry is never in tension**, leading to zero failure by mechanical interaction during irradiation.

With the CEGA PyC data, the SiC layer of the particle is in tension before EOL for the HFR-K3/3 pebble and a simple statistical analysis leads to less than one failed particle. While taking CEGA properties is not justified because these properties are in principle more adapted to US particles than to German's, this failure value is not inconsistent with the irradiation results.

This results are to be compared with CONVOL and STRESS3 results in the complete document (deliverable n°3.3).



REFERENCES

- [1] Note technique SESC/LSC 04-021 indice 0
Notice de présentation d'ATLAS V1.0
F.Michel

- [2] Note technique HTR-F1-04/08-D-3.2.1 first version
Selection of benchmark cases for mechanical failure prediction
H. Nabielek, K. Verfondern, H.Werner

- [3] Note technique HTR-F-03/12-D-3.2.1 first version
Selection of properties and models for the HTR coated particle – HTR-F WP3 deliverable n°12
A collaboration of work performed by CEA, FRAMATOME/ ANP, FZJ and BNFL
M. Pelletier, P. Guillermier, H. Nabielek, T. Abram

- [4] Note technique SESC/LIAC 03-019 (HTR-F-03/11-D-3.4.1) indice 0
HTR-F project – Deliverable n°13 – ATLAS first calculations
Guy Degenève, M.Phélip



LIST OF TABLES

TABLE 1 : SUMMARY OF HFR-K3 IRRADIATION RESULTS	13
---	----



TABLE 1 : SUMMARY OF HFR-K3 IRRADIATION RESULTS

Sphere Number	Centre Temperature (°C)	Burn-up %FIMA	Fast Neutron Dose E>0.1 MeV (x 10 ²⁵ m ⁻²)	R/B			
				BOL		EOL	
				Kr 85m	Kr 88	Kr 85m	Kr 88
HFR-K3/1	1200	7.5	4.0	1.0 x 10 ⁻⁹	-	2.0 x 10 ⁻⁷	-
HFR-K3/2	920	10.0	5.8	9.0 x 10 ⁻¹⁰	-	1.0 x 10 ⁻⁷	-
HFR-K3/3	920	10.6	5.9	9.0 x 10 ⁻¹⁰	-	1.0 x 10 ⁻⁷	-
HFR-K3/4	1220	9.0	4.9	2.0 x 10 ⁻⁹	-	3.0 x 10 ⁻⁷	-



LIST OF FIGURES

FIGURE 1 : HFR-K3 IRRADIATION TEST _____	15
FIGURE 2 : HFR-K3 CAPSULE 1 _____	16
FIGURE 3 : THERMAL RESULTS – $T = f(T)$ _____	17
FIGURE 4 : MECHANICAL RESULTS – TANGENTIAL STRESSES _____	18
FIGURE 5 : PRESSURE IN THE PARTICLE _____	19
FIGURE 6 : CEGA IRRADIATION INDUCED DIMENSIONAL CHANGE AND CREEP CONSTANT _____	20
FIGURE 7 : STATISTICAL APPROACH _____	21

FIGURE 1 : HFR-K3 IRRADIATION TEST

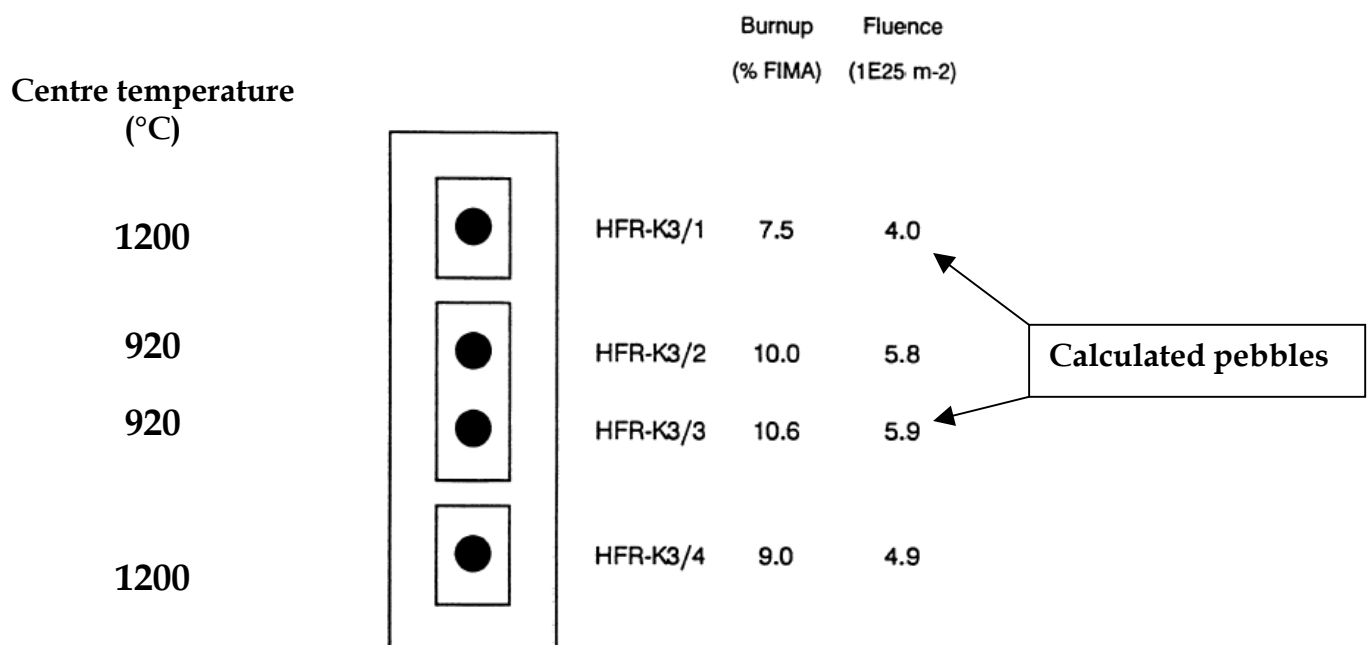
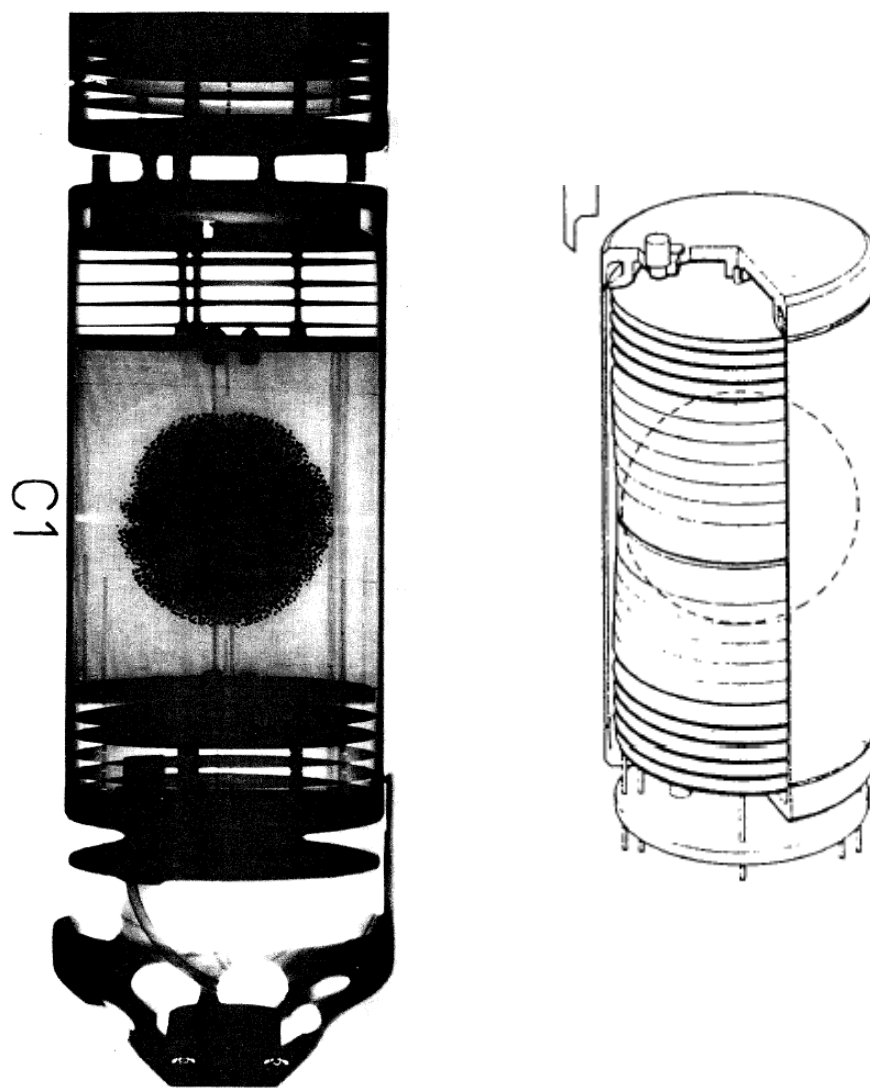


FIGURE 2 : HFR-K3 CAPSULE 1

Radiograph of the capsule

FIGURE 3 : THERMAL RESULTS – $T = f(T)$

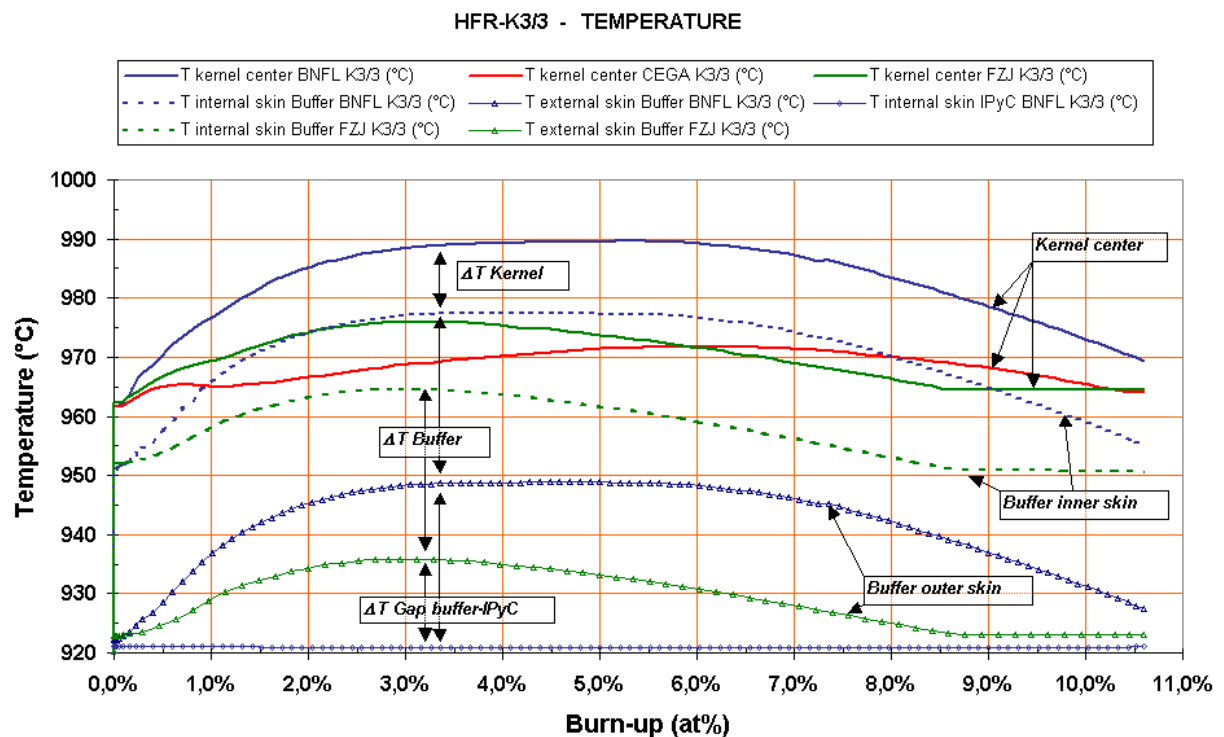
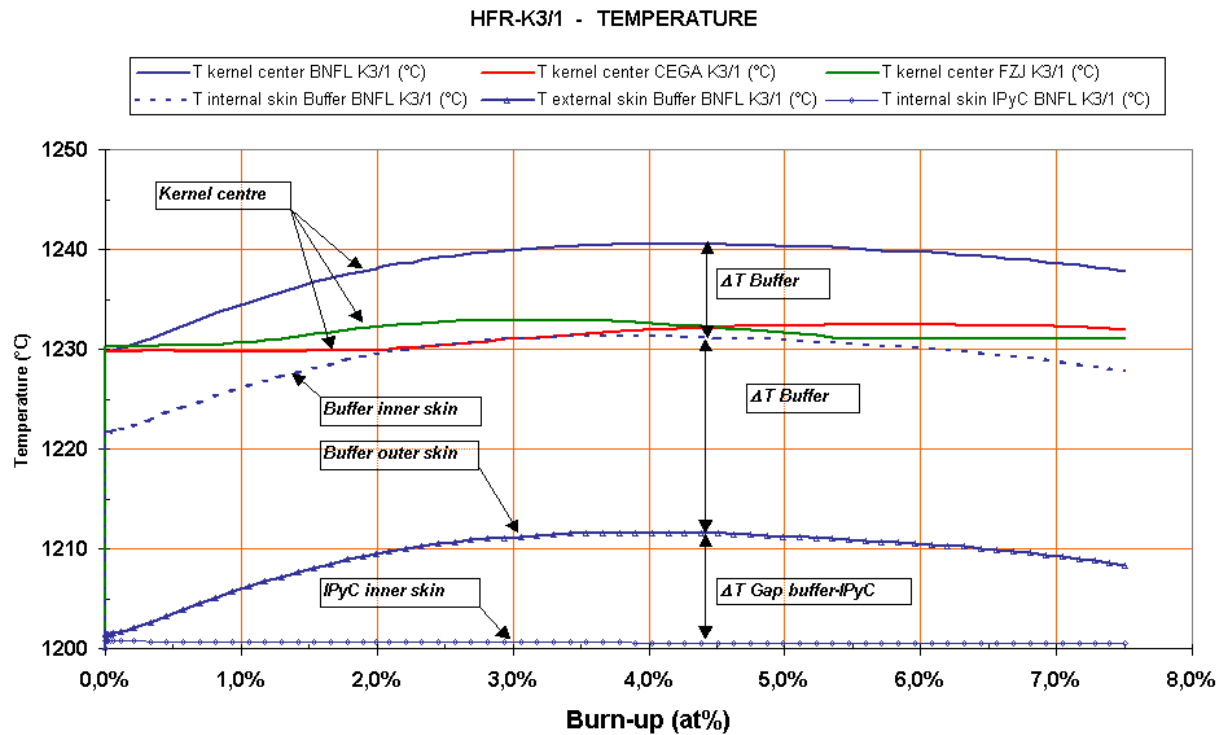
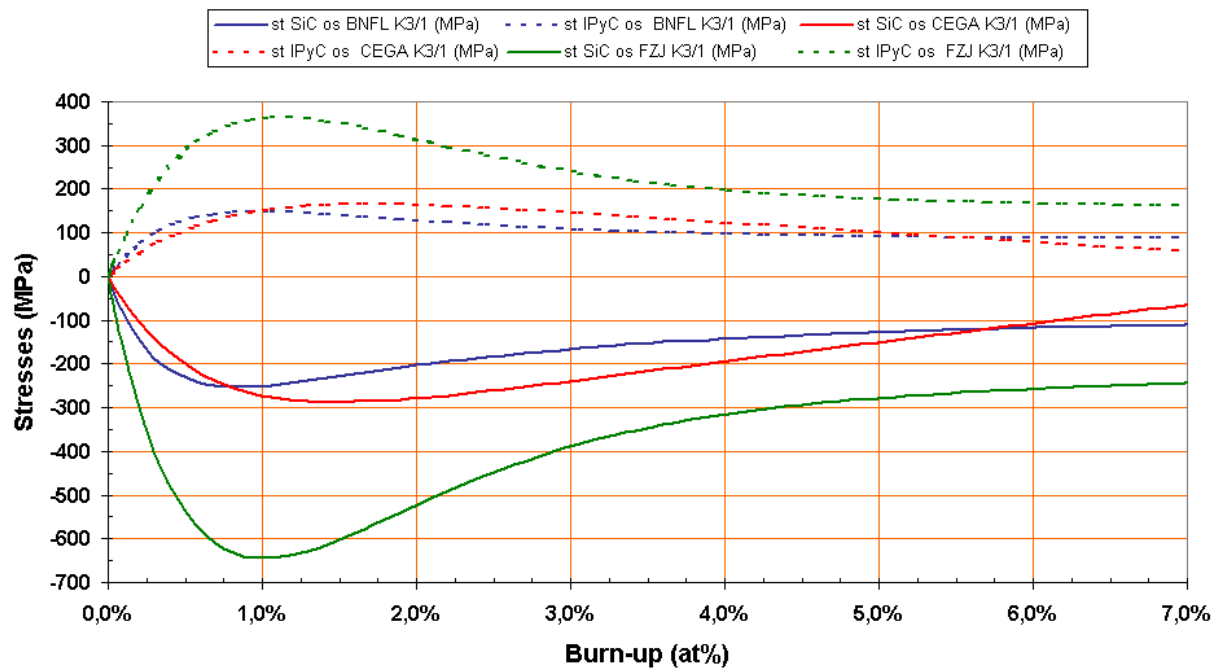


FIGURE 4 : MECHANICAL RESULTS – TANGENTIAL STRESSES

HFR-K3/1



HFR-K3/3

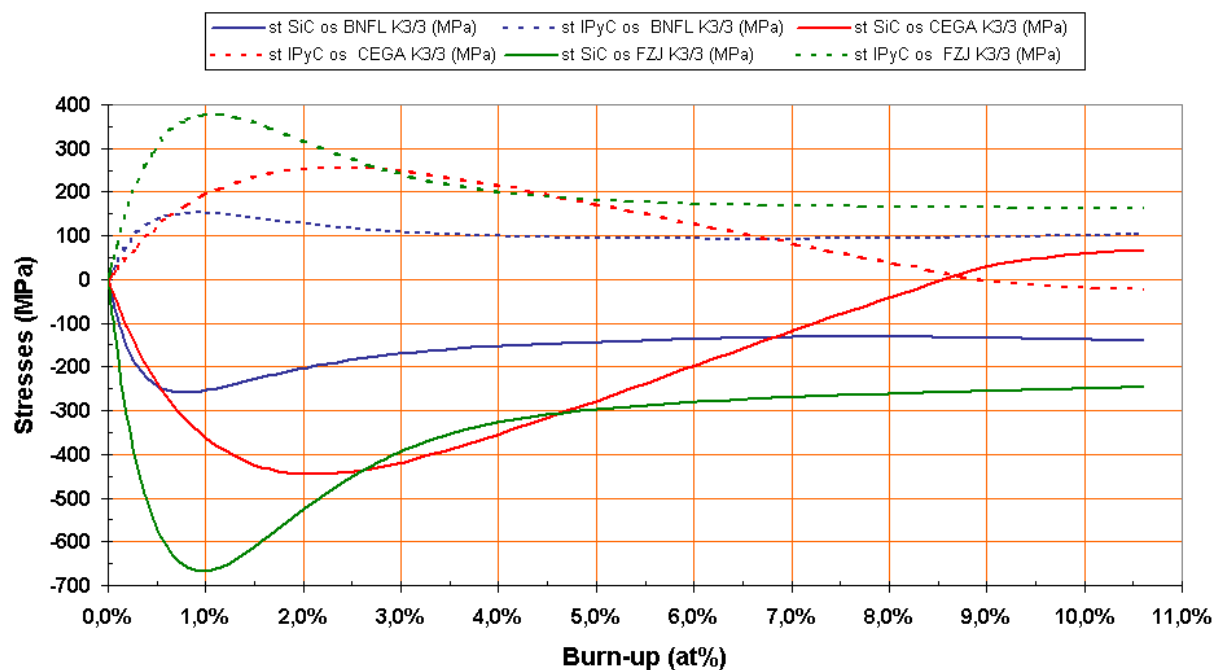


FIGURE 5 : PRESSURE IN THE PARTICLE

HFR-K3/1 and HFR-K3/3 - Pressure

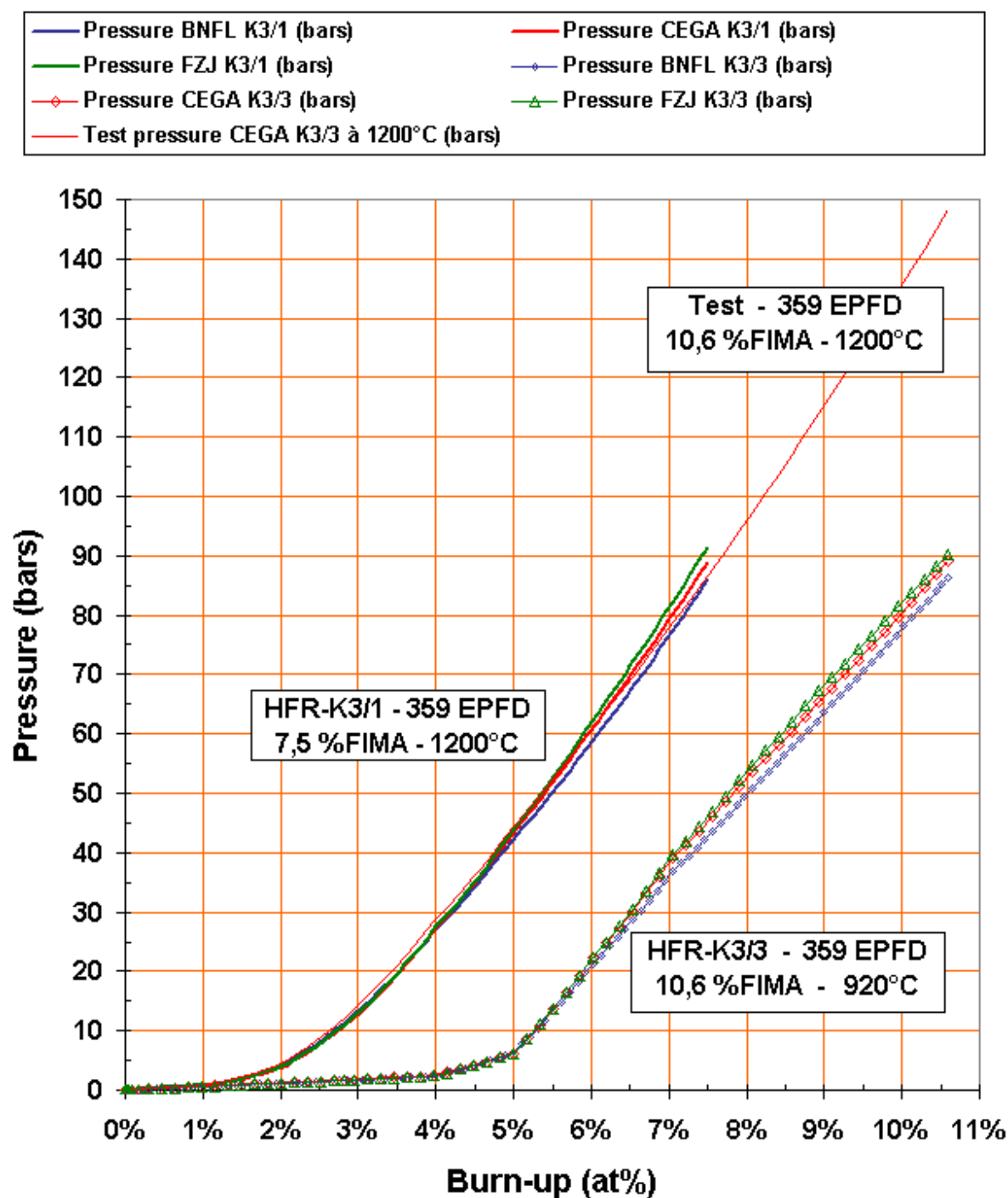
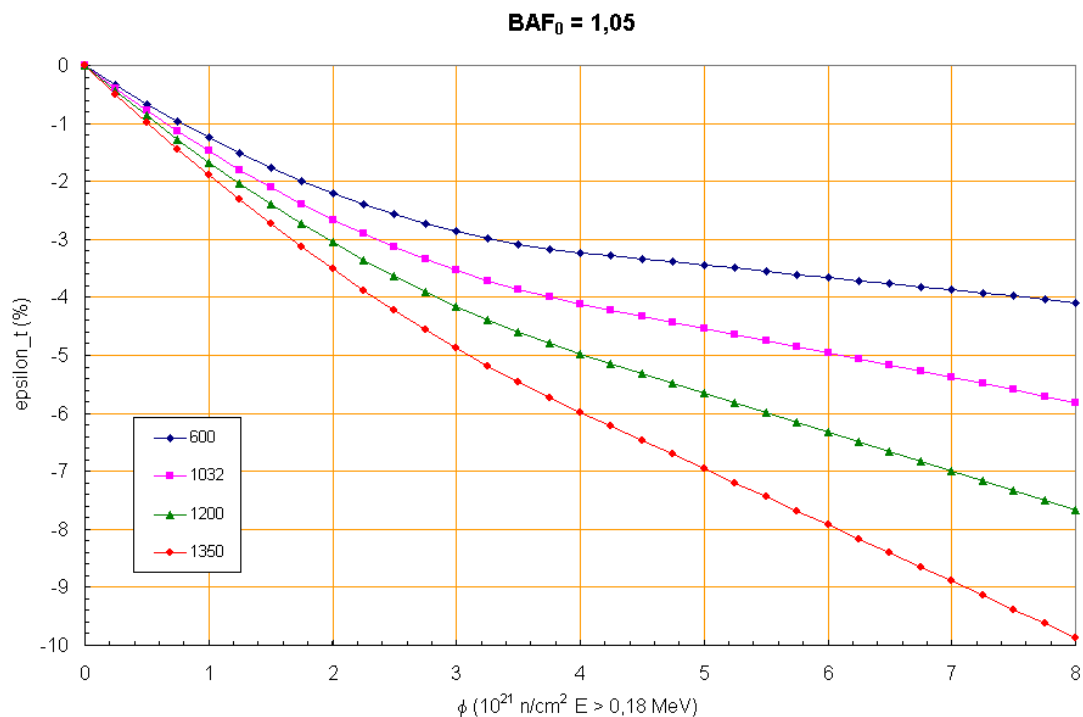


FIGURE 6 : CEQA IRRADIATION INDUCED DIMENSIONAL CHANGE AND CREEP CONSTANT



Irradiation induced creep constant K

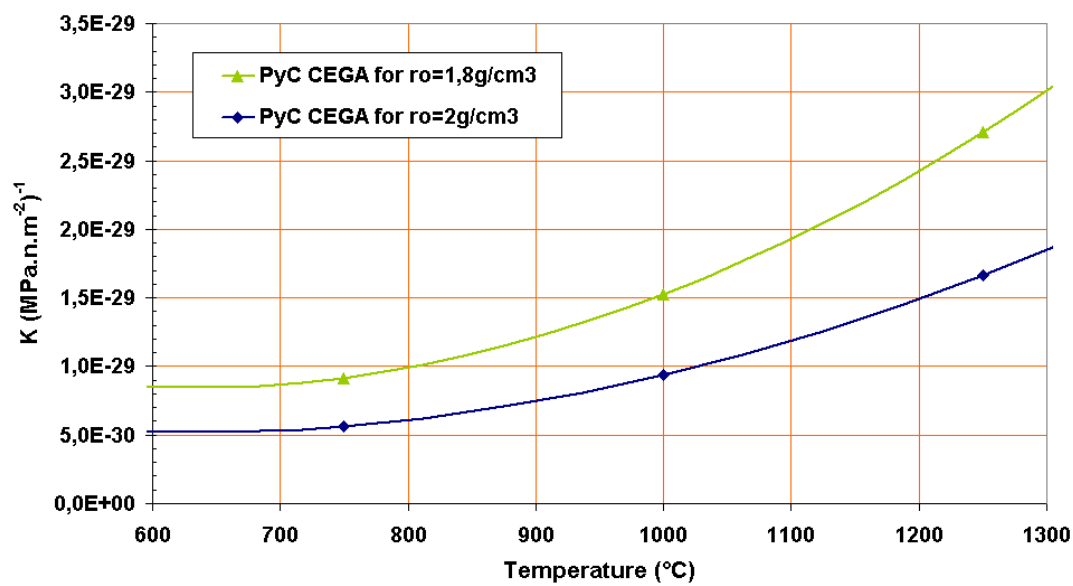
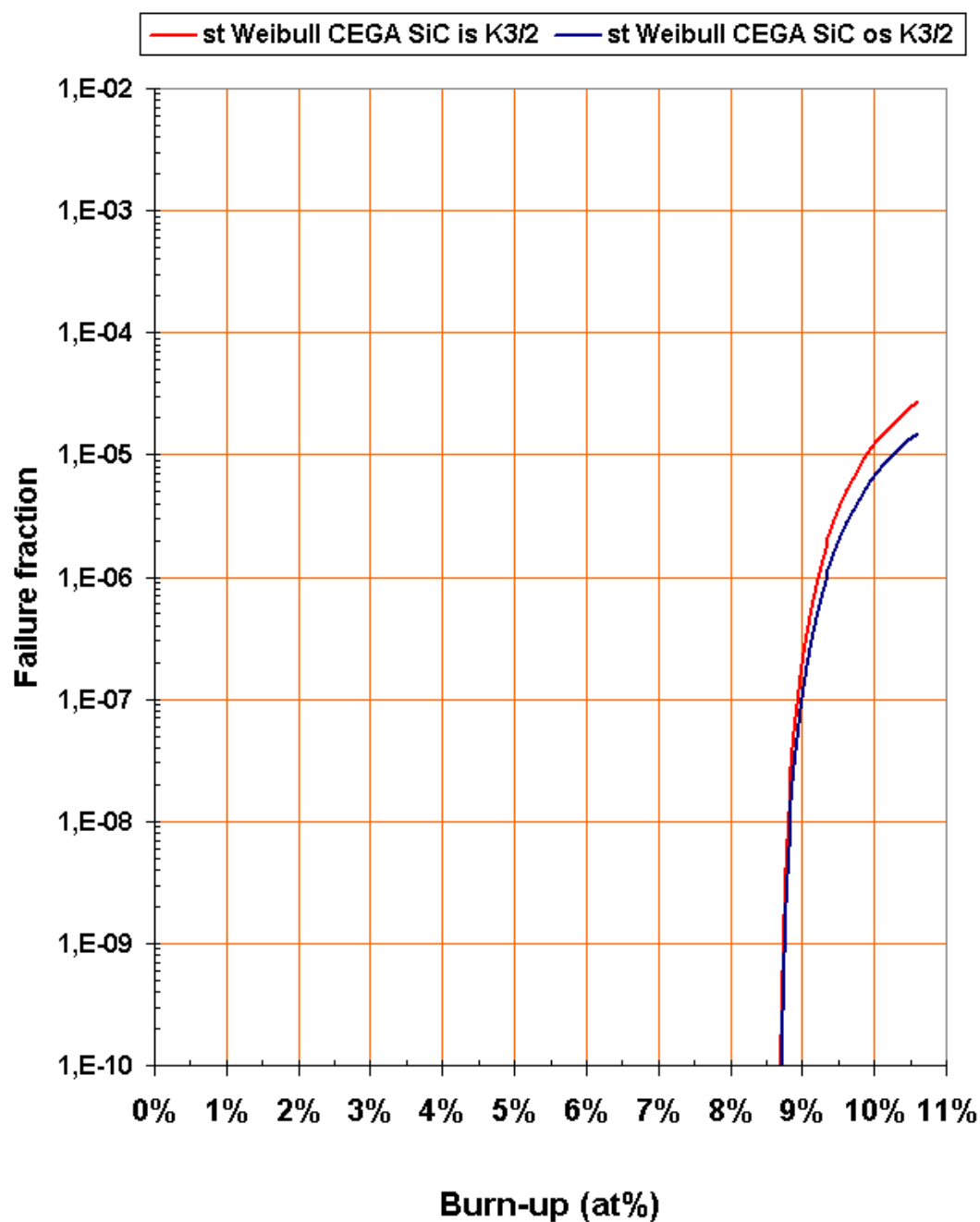


FIGURE 7 : STATISTICAL APPROACH

HFR-K3/1 - CEGA properties - Failure fraction





LIST OF ANNEXES

ANNEX A : HFR-K3/1 ATLAS LISTING	23
----------------------------------	----



ANNEX A: HFR-K3/1 ATLAS LISTING

```
***** MAILLAGE Cas 10 HFR-K3B2
Type de maillage [mot cl, '1D' , '2Dcentre' ou '2D'] d,faut '2D'
'1D'
Nb de couches (en plus du combustible) et numero de la couche subissant le pression interne
4 2
rayon noyau (m) et nb de mailles suivant le rayon
248.5E-6 6
Jeux entre couches (n-1) et n : n (entier) et valeur initiale du jeu (m) (de 0 ... n lignes)3 0E-6
1 0.2E-6
2 0.2E-6
epaisseur minimale des jeux entre couches (2.E-7 conseil,) (m)
2.E-7
epaisseur couches (m) et nb de mailles dans l'epaisseur (autant de lignes que de couches)
94.E-6 6
41.E-6 5
36.E-6 5
40.E-6 5
nombres de portions divisant pi/2 radians du maillage spherique
12
*
***** MATERIAUX
Noyau : Materiau (mot), porosite, (/)
UO2 0.0128
Noyau : enrichissement (en Pu ou U5) (/), taille des grains (m), stoechiometrie O/M (/)
0.0982 1.E-6 2.006
Fission : Energie et unit, [mot:'J/mol' ou eV ou MeV]
200. MeV
Gaz atoms per fission : 'name' and rate (/)
'Xe' 0.301
Couches : mat,riau (MOT) et porosite, (/)
'LAB' 0.559
'PyC_BNFL' 0.172
'SiC_CEA' 0.012
'PyC_BNFL' 0.172
Part des porosites ouvertes dans le noyau et dans le buffer (couche 1)
0. 1.
Gaz interne ... la particule de fabrication (mot cl,:XE) et pression (en Pa)
'Xe' 1.
***** conditions speciales (voir notice)
'BAF' 2 '==' 1.053
'BAF' 4 '==' 1.019
* * * *
***** additional outputs
'AF1' 'EXTERIEUR' 2
'DENT' 'INTERIEUR' 1
'DENT' 'INTERIEUR' 2
* * * *
***** HISTORIQUE D'IRRADIATION *****
Pression exterieure (en Pa)
1.E5
flu neutronique nominal (valeur et MOT cl, unit, 'n/m2/s' ou 'mol/m2/s', avec les cotes'')
1.29E18 'n/m2/s'
proba de fission=d[FIMA]/dt nominale (s-1)
2.41798E-9
*** Nombre de pas donnees (autres que t=0), les valeurs au del... ne seront pas lues
5
*** temps max d'une iteration (s) et multipleur (les iterations rajoutees seront ... flu lineairement
interpol,ee)
500000. 2
*** mode de calcul du flu neutronique : Mot cl, (PROP ou X)
PROP
*** Historique t (s), temperature ext,rieure (K), evolution norme de la proba de fission , si besoin
evolution norme de la fluence (dans le cas fluence non PROP), il faut de 3 ou 4 valeurs par ligne
0. 1473. * t=0. , pour ce temps seule la temperature est lue
60. 1473. 1.
86400. 1473. 1.
864000. 1473. 1.
8640000. 1473. 1.
31017600. 1473. 1.
```